

# Quantitation of eleven alkyl amines in atmospheric samples: Separating structural isomers by ion chromatography

B. K. Place<sup>1, 2</sup>, A. T. Quilty<sup>2</sup>, R. A. Di Lorenzo<sup>1</sup>, S. E. Ziegler<sup>2</sup> and T. C. VandenBoer<sup>2</sup>

<sup>1</sup>Department of Chemistry, Memorial University, St. John's, NL, Canada

<sup>2</sup>Department of Earth Sciences, Memorial University, St. John's, NL, Canada

Correspondence to: T. C. VandenBoer (tvandenboer@mun.ca)

**Abstract:** Amines are important drivers in particle formation and growth, which has implications for Earth's climate. In this work, we developed an ion chromatographic (IC) method using sample cation-exchange preconcentration for separating and quantifying the nine most abundant atmospheric alkyl amines (monomethylamine (MMAH<sup>+</sup>), dimethylamine (DMAH<sup>+</sup>), trimethylamine (TMAH<sup>+</sup>), monoethylamine (MEA<sup>+</sup>), diethylamine (DEAH<sup>+</sup>), triethylamine (TEAH<sup>+</sup>), monopropylamine (MPAH<sup>+</sup>), isomonopropylamine (iMPAH<sup>+</sup>), and monobutylamine (MBAH<sup>+</sup>)) and two alkyl diamines 1, 4-diaminobutane (DABH<sup>+</sup>) and 1, 5-diaminopentane (DAPH<sup>+</sup>). Further, the developed method separates the suite of amines from five common atmospheric inorganic cations (Na<sup>+</sup>, NH<sub>4</sub><sup>+</sup>, K<sup>+</sup>, Mg<sup>2+</sup>, Ca<sup>2+</sup>). All 16 cations are greater than 95% baseline resolved and elute in a runtime of 35 minutes. This paper describes the first successful separation of DEAH<sup>+</sup> and TMAH<sup>+</sup> by IC and achieves separation between three structural isomer pairs, providing specificity not possible by mass spectrometry. The method detection limits for the alkyl amines are in the picogram per injection range and the method precision ( $\pm 1\sigma$ ) analyzed over 3 months was within 16 % for all the cations. The performance of the IC method for atmospheric application was tested with biomass-burning (BB) particle extracts collected from two forest fire plumes in Canada. In extracts of size-resolved BB samples from an aged plume we detected and quantified MMAH<sup>+</sup>, DMAH<sup>+</sup>, TMAH<sup>+</sup>, MEAH<sup>+</sup>, DEAH<sup>+</sup> and TEAH<sup>+</sup> in the presence of Na<sup>+</sup>, NH<sub>4</sub><sup>+</sup>, and K<sup>+</sup> at amines to inorganic cations molar ratios ranging from 1:2 to 1:1000. Quantities of DEAH<sup>+</sup> and DMAH<sup>+</sup> of 0.2 – 200 ng m<sup>-3</sup> and 3 – 1200 ng m<sup>-3</sup>, respectively, were present in the extracts and an unprecedented amines to ammonium molar ratio greater than one was observed in particles with diameters spanning 56 – 180 nm. Extracts of respirable fine mode particles (PM<sub>2.5</sub>) from a summer forest fire in British Columbia in 2015 were found to contain iMPAH<sup>+</sup>, TMAH<sup>+</sup>, DEAH<sup>+</sup> and TEAH<sup>+</sup> at molar ratios of 1:300 with the dominant cations. The amines to ammonium ratio in a time-series of samples never exceeded 0.15 during the sampling of the plume. These results and an amines standard addition demonstrate the robustness and sensitivity of the developed method when applied to the complex matrix of biomass burning particle samples. The detection of multiple alkyl amines in the analyzed BB samples indicates that this speciation and quantitation approach can be used to constrain BB emission inventories and the biogeochemical cycling of these reduced nitrogen species.

1    **1    Introduction**

2    Particles in the atmosphere can modulate climate through their direct and indirect effect on the radiative balance  
3    of Earth's atmosphere (Boucher et al., 2013; Lohmann and Feichter, 2005). This potential warming or cooling  
4    effect of particles represents the greatest uncertainty in Earth's radiative forcing (Myhre et al., 2013). Additionally,  
5    particles with a diameter of 2.5  $\mu\text{m}$  or less (PM<sub>2.5</sub>) have been classified as carcinogens (IARC, 2016), and are  
6    estimated to be responsible for 3 million deaths annually worldwide (Stephen et al., 2012). Thus understanding  
7    the quantities, and the chemical and physical nature of the species involved in the formation and growth of new  
8    particles is of paramount importance.

9    Recent work has shown that organic compounds may contribute considerably to particle nucleation (Ehn et al.,  
10   2014; Ortega et al., 2016; Tröstl et al., 2016; Willis et al., 2016). In particular, the need to measure and quantify  
11   gaseous atmospheric alkyl amines has gained interest because of their exceptional ability to partake in atmospheric  
12   particle formation. Multiple laboratory investigations have shown the nucleation potential of methyl- and ethyl-  
13   substituted amines through gaseous acid-base chemistry reactions (Almeida et al., 2013; Angelino et al., 2001;  
14   Berndt et al., 2010; Berndt et al., 2014; Bzdek et al., 2010; Bzdek et al., 2011; Erupe et al., 2011; Jen et al., 2016a;  
15   Jen et al., 2016b; Lloyd et al., 2009; Murphy et al., 2007; Qiu et al., 2011; Silva et al., 2008; Smith et al., 2010;  
16   Wang et al., 2010a; Wang et al., 2010b; Yu et al., 2012; Zhao et al., 2011; Zollner et al., 2012). Theoretical  
17   calculations and studies have also found that amines have a high disposition to form atmospheric nanoparticles  
18   (Barsanti et al., 2009; Kurtén et al., 2008; Loukonen et al., 2014; Loukonen et al., 2010; Nadykto et al., 2015;  
19   Ortega et al., 2012). From these works, alkyl amines have been shown to form clusters via neutralization reactions  
20   at rates up to three orders of magnitude greater than ammonia (Almeida et al., 2013; Berndt et al., 2010; Bzdek et  
21   al., 2011; Kurtén et al., 2008; Loukonen et al., 2010; Nadykto et al., 2015), and readily exchange with ammonia  
22   in already formed ammonium-bisulfate molecular clusters (Bzdek et al., 2010; Lloyd et al., 2009; Qiu et al., 2011).  
23   These studies suggest that alkyl amines can compete with ammonia to form particles even though they have been  
24   quantified at mixing ratios that are three or more orders of magnitude less in the atmosphere (Chang et al., 2003;  
25   Ge et al., 2011; Schade and Crutzen, 1995). Atmospheric measurements made during new particle formation  
26   events have further confirmed that alkyl amines participate in particle formation at ambient concentrations and  
27   that these species may be present in most atmospheric particles (Creamean et al., 2011; Dall'Osto et al., 2012;  
28   Hodshire et al., 2016; Kulmala et al., 2013; Kürten et al., 2016; Ruiz-Jimenez et al., 2012; Smith et al., 2010; Tao  
29   et al., 2016).

30   Alkyl amine emissions to the atmosphere arise from both natural and anthropogenic sources (Ge et al., 2011).  
31   Short-chain alkyl amines such as the methylated and ethylated amines are predominantly reported in emission  
32   inventories. Measurements show that atmospheric alkyl amines are prevalent in ambient air across the globe,  
33   especially in the particle phase (Ge et al., 2011). For example, methyl and ethyl amines were measured by an  
34   aerosol time-of-flight mass spectrometer (AToFMS) at both rural and urban sites all across Europe (Healy et al.,  
35   2015). In particular, these amines have been measured in substantial quantities near animal husbandry operations  
36   (Kuhn et al., 2011; Lunn and Van de Vyver, 1977; Rabaud et al., 2003; Schade and Crutzen, 1995; Sorooshian et  
37   al., 2008), fisheries (Seo et al., 2011), and sewage-waste treatment facilities (Leach et al., 1999). Other  
38   anthropogenic sources include tobacco smoke (Schmeltz and Hoffmann, 1977), automobiles (Cadle and Mulawa,  
39   1980) and cooking (Rogge et al., 1991; Schauer et al., 1999). The ocean is estimated to be the largest natural source

1 of alkyl amines, where they are released as volatile degradation products (Ge et al., 2011; Gibb et al., 1999a; Gibb et al., 1999b). Aliphatic amines have also been detected in smoldering stage biomass burning plumes. These have been estimated to represent a quarter of global methylated amine emissions (Lobert et al., 1990; Schade and Crutzen, 1995).

5 Real-time in-situ speciation and quantitation of atmospheric amines in the particle and gas phase can be difficult  
6 because alkyl amines are commonly found at or below parts per trillion by volume (pptv) mixing ratios in the  
7 atmosphere (Ge et al., 2011). Furthermore, the atmospheric matrix can be complex and ubiquitous atmospheric  
8 species can cause matrix effects for various analytical methods targeting these reduced nitrogen species. Being  
9 able to chromatographically resolve alkyl amines from the dominant base, ammonium, represents a major  
10 challenge when sampling the gas phase (Chang et al., 2003; Ge et al., 2011; Schade and Crutzen, 1995).  
11 Quantifying amines in particle samples, for example by ion chromatography, presents a greater challenge due to  
12 possible interferences from sodium, potassium, ammonium, magnesium and calcium whose concentrations are  
13 dependent on the particle source characteristics and the measurement location (Ault et al., 2013; Kovac et al.,  
14 2013; Sobanska et al., 2012; Sun et al., 2006). Particles frequently contain complex organic mixtures, such as high  
15 molecular weight organic compounds, which can cause further matrix effects during separation or direct analysis  
16 (Di Lorenzo and Young, 2016; Saleh et al., 2014).

17 Achieving full speciation of alkyl amines is important because the nucleation potential of amines has been shown  
18 to increase with basicity (Berndt et al., 2014; Kurtén et al., 2008; Yu et al., 2012). For example, although  
19 monopropylamine (MPA) and trimethylamine (TMA) are structural isomers of one another, MPA is likely to be a  
20 more potent nucleator due to its stronger basicity. The suite of alkyl amines that have been commonly detected in  
21 the atmosphere contains multiple structural isomers (e.g. monoethylamine (MEA) and dimethylamine (DMA)),  
22 making it difficult to speciate the amines using mass spectrometry (MS) without prior separation. Multiple field  
23 investigations sampling atmospheric particles using MS analysis have reported the detection of amine ion peaks  
24 but have been unable to assign them to a specific amine (Aiken et al., 2009; Denkenberger et al., 2007; Silva et  
25 al., 2008; Yao et al., 2016). Derivatization of alkyl amines coupled with HPLC or GC separation has been reported  
26 to aid in separation and quantitation of amine species (Akyüz, 2007; Huang et al., 2009; Fournier et al., 2008; Key  
27 et al., 2011; Possanzini and Di Palo, 1990). However, these approaches are time consuming, require optimization  
28 of reaction conditions, and employ phase separations, which use large quantities of consumables, reagents, and  
29 solvents. Capillary electrophoresis has also been employed for aqueous amine separation, however in either case  
30 derivatization was required (Dabek-Złotorzynska and Maruszak, 1998) or the separation of atmospherically  
31 relevant cations was not addressed (Fekete et al., 2006). The use of ion chromatography to directly separate and  
32 quantify atmospheric alkyl amines has been demonstrated (Chang et al., 2003; Dawson et al., 2014; Erupe et al.,  
33 2010; Huang et al., 2014; Li et al., 2009; Murphy et al., 2007; VandenBoer et al., 2012; Verrielle et al., 2012), yet  
34 the established IC methods struggle with coeluting cations (Huang et al., 2014; Murphy et al., 2007; VandenBoer  
35 et al., Verrielle et al., 2012) or they do not address a full suite of atmospherically relevant alkyl amines and inorganic  
36 cations (Chang et al., 2003; Dawson et al., 2014; Erupe et al., 2010; Li et al., 2009).

37 In this work we demonstrate the separation and quantitation of the nine most abundant atmospheric alkyl amines,  
38 two alkyl diamines, and six inorganic cations through the use of ion chromatography. We show i) the separation  
39 method approach to maximizing peak resolution in the context of real-time atmospheric sampling and analysis; ii)

1 the effects of column temperature on amine coelution; iii) the method precisions, accuracies, sensitivities and  
2 limits of detection (LODs) for all alkyl amine and inorganic cations; and iv) application of the method to the  
3 complex matrix of atmospheric biomass burning particle extracts to demonstrate method sensitivity and  
4 robustness.

5

6 **2 Methods**

7 **2.1 Chemicals and materials**

8 Inorganic cation stock solutions were prepared from a primary mixed cation standard concentrate (Dionex six-  
9 cation II, Lot #150326, Thermo Scientific, Waltham, MA, USA) consisting of  $\text{Li}^+$ ,  $\text{Na}^+$ ,  $\text{NH}_4^+$ ,  $\text{K}^+$ ,  $\text{Mg}^{2+}$  and  $\text{Ca}^{2+}$   
10 chloride salts. Alkyl amines (MMA (monomethylamine, 40% w/w), DMA (dimethylamine, 40% w/w), TMA  
11 (trimethylamine, 25 % w/w), MEA (monoethylamine, 70 % w/w), DEA (diethylamine, >99% w/w), TEA  
12 (triethylamine, >99% w/w), MPA (monopropylamine,  $\geq$  99% w/w), iMPA (isomonopropylamine,  $\geq$  99% w/w)  
13 MBA (monobutylamine, 99.5% w/w), MEtA (monoethanolamine,  $\geq$  98% w/w), DAB (1,4-diaminobutane,  
14 >98.5% w/w) and DAP (1,5-diaminopentane, 95% w/w)) were purchased from Sigma-Aldrich (Oakville, ON,  
15 Canada). Calibration standards were prepared by serial dilution in 18.2  $\text{M}\Omega$  ultrapure deionized water (Barnstead  
16 Nanopure Infinity, Thermo Scientific, Waltham, MA, USA). Since these alkyl amine species will largely be  
17 protonated in solution we will denote each of these species in their cationic form (i.e.  $\text{NR}_3\text{H}^+$ ) henceforth when  
18 referring to the condensed phase.

19 **2.2 Ion Chromatography**

20 A ThermoScientific ICS-2100 Ion Chromatography System (Thermo Scientific, Mississauga, ON, Canada)  
21 utilizing Reagent-Free Ion Chromatography (RFIC<sup>TM</sup>) components was used to develop the separation of the  
22 selected amines and inorganic cations. A ThermoScientific methanesulfonic acid (MSA) eluent generator cartridge  
23 (EGC III, P/N: 074535) was used in conjunction with an ultrapure deionized water reservoir to supply the eluent  
24 mobile phase with  $\text{H}_3\text{O}^+$  ions as the competing exchanger. A continuously regenerated trap column (CR-CTC II,  
25 P/N: 066262) was attached in series to the eluent cartridge to remove cation contaminants from the eluent, thereby  
26 improving instrument detection limits. Samples were preconcentrated on a cation exchange column (TCC-ULP1;  
27 5 x 23 mm, P/N: 063783) using a ThermoScientific AS-DV autosampler to deliver the desired volume.  
28 Concentrated analytes were separated using ThermoScientific CG19 (4 x 50 mm, P/N: 076027) and CS19 (4 x 250  
29 mm, P/N: 076026) guard and analytical cation-exchange columns. The column effluent was passed through a  
30 suppressor operating in recycle mode (CERS 500, 4 mm) prior to detection of the analytes using a DS6 heated  
31 conductivity cell thermostated at 30 °C. The eluent conductance was recorded at 5 Hz and the chromatographic  
32 peaks were analyzed using the Chromeleon<sup>TM</sup> 7 software package. A ThermoScientific CG15 (4 x 50 mm, P/N:  
33 052200) guard column was added in-line later to attempt further improvement in analyte separation.

1    **2.3 CS19 separation optimization**

2    The gradient program used for the separation of methylamines, ethylamines, other alkyl amines and six inorganic  
3    cations on the CS19 cation-exchange column was optimized by combining analyte separation parameters from  
4    multiple isocratic elution runs at varying MSA concentrations (1 - 16 mM) and mobile phase flow rates (0.75 -  
5    1.25 ml min<sup>-1</sup>) at a column temperature of 30 °C. Maximum peak resolution was optimized using an eluent gradient  
6    program and the column temperature was increased to resolve co-eluting peaks (see Sect. 3.1.1).

7    Optimal separation of a suite of 15 cations was achieved using a mobile phase flow rate of 1.25 ml min<sup>-1</sup> and a  
8    column temperature of 55 °C. The eluent gradient program is as follows: an initial MSA concentration of 1 mM  
9    held for 20 minutes, a step increase to 4 mM followed immediately by an exponential ramp to 10 mM over 10  
10   minutes (Chromeleon curve factor = 7). The final concentration of 10 mM was held for an additional 5 minutes,  
11   yielding a total run time of 35 minutes. The IC was returned to initial conditions and re-equilibrated **for 10 minutes**  
12   as the next **1 ml sample aliquot** was prepared for injection by the AS-DV. **The suppressor current, optimized for**  
13   **this flow rate and the maximum eluent concentration in accordance with the calculation provided by the**  
14   **manufacturer, was set at 37 mA. The typical backpressure in the system at these conditions was 2100 psi. The**  
15   **Chromeleon method file for the method described above is detailed in Fig. S1.**

16    **2.4 Quality Assurance and Quality Control**

17   Standards were prepared using Class A Corning polymethylpentene 50 ( $\pm 0.06$ ) ml volumetric flasks that were  
18   rinsed 4 times with ethanol and 8 times with ultrapure water prior to use. Standards were stored in 60 ml brown  
19   Nalgene polypropylene bottles that were pre-cleaned in a 10 % HCl bath, followed by 8 sequential rinses with  
20   distilled and ultrapure water, respectively. The mixed amine standards and mixed inorganic cation standards were  
21   prepared separately and each cation standard set was composed of five calibration standards, two check standards  
22   **and an ultrapure deionized water blank**. Ranges and related parameters are denoted by mass injected, as the  
23   preconcentration column negates the effect of volume. All amine calibration standards had a mass calibration range  
24   of 5-500 ng. The mass range for each inorganic cation calibration is as follows: Li<sup>+</sup> (0.82-16 ng), Na<sup>+</sup> (7.8-160  
25   ng), NH<sub>4</sub><sup>+</sup> (8.4-170 ng), K<sup>+</sup> (26-520 ng), Mg<sup>2+</sup> (6.4-130 ng), and Ca<sup>2+</sup> (18-360 ng). **All calibration curves contained**  
26   **trace inorganic cation impurities from the ultrapure deionized water source or holding vessels that fell below the**  
27   **lowest calibration standard, and were corrected accordingly to allow for inter-day method performance**  
28   **comparison. Trace quantities of amines were not observed. An example of a calibration blank chromatogram is**  
29   **presented in Fig. S2.**

30   Method precision for each methyl and ethyl amine cation was determined using standard calibration curves ( $n =$   
31   9) injected across five different days spanning three months. The precision for the propyl and butyl amines was  
32   determined using two standard calibration curves analyzed over one month. Method precision for Li<sup>+</sup>, Na<sup>+</sup>, NH<sub>4</sub><sup>+</sup>  
33   and K<sup>+</sup> was assessed using calibrations ( $n = 6$ ) from three separate days spanning two months. Precision for each  
34   cation was calculated using the standard deviation ( $\sigma$ ) in the slope of the linear calibration curves. Check standards  
35   positioned between the two highest and the two lowest calibration standards for each cation were used to determine  
36   method accuracy across the calibration range. The low check standard was 15 times greater than the lowest standard  
37   and the high check standard was 150 times higher than the lowest standard. Accuracy was determined by

1 the percent relative error between the known and calculated concentrations of the check standards. The limits of  
2 detection (LOD) for the singly-charged inorganic cations ( $n = 4$ ) and methyl and ethyl amines ( $n = 5$ ) were  
3 determined using calibration standard and calibration blank chromatograms from three or more separate days. The  
4 LODs for the propyl and butyl amines were determined using calibration standard and blank chromatograms from  
5 two separate days. The LODs are reported as concentrations resulting in a signal peak height to background noise  
6 ratio of three. The background noise was determined using the standard deviation of the conductance signal that  
7 fell within the retention time window for each analyte in their respective calibration blank chromatograms.

8 To assess the method robustness in the presence of a complex matrix the gradient method standard addition was  
9 performed on a subsample of a size-resolved BB particle extract (320 – 560 nm) (see Sect 2.5). Standard addition  
10 was performed by adding known quantities of methyl and ethyl amine solution to a 0.5 ml sample of the extract  
11 followed by dilution to 5 ml. The amount of the methyl and ethyl amines added to the internal calibration matched  
12 that of the external calibration. The slope and retention times for the methyl and ethyl amines from the internal  
13 calibration were calculated and compared to those performed externally to quantify matrix effects. Discussion of  
14 the analytical performance of the CS19 gradient program is presented in Sect. 3.1.2.

## 15 **2.5 Size-resolved BB sample analysis**

16 A size-resolved particle sample from a BB plume was collected using a nanoMOUDI II (nano micro-orifice  
17 uniform-deposit impactor, model 122-R, MSP Corp., Shoreview, MN, USA) in St. John's, Newfoundland on July  
18 6, 2013. Satellite images of the plume smoke, HYSPLIT back trajectories, as well as, measured PM<sub>2.5</sub>  
19 concentrations reported by Environment and Climate Change Canada indicate that these plumes originated from  
20 boreal forest fires in northern Quebec and Labrador on July 4, 2013 and travelled via Labrador and the Gulf of St.  
21 Lawrence to the sampling site (Di Lorenzo and Young, 2016). The nanoMOUDI samples were collected on 13  
22 aluminum substrate stages into size-resolved bins of atmospheric particles with a diameter range spanning 0.010  
23 – 18  $\mu\text{m}$ . Air was sampled continuously for 25.5 hours at a flow rate of 30 L min<sup>-1</sup>. A sub-sample of each aluminum  
24 substrate (10 % of the total substrate area) was extracted into a glass vial with 5 mL ultrapure deionized water by  
25 sonication (VWR Scientific Products/Aquasonic 150HT, Ultrasonic Water Bath) for 40 minutes. The extracts were  
26 filtered using a 0.2  $\mu\text{m}$  polytetrafluoroethylene (PTFE) filter and stored in polypropylene vials at 4 °C prior to  
27 analysis by IC within 24 hours. Cation analytes within these samples all fell within their respective calibration  
28 ranges and did not require any further dilution. An aluminum substrate field blank was also transported and  
29 exposed to the ambient atmosphere briefly at the collection site before being stored in a sealed container for the  
30 duration of the sample collection, transported back with the samples, and extracted simultaneously following the  
31 same procedure. All calculated quantities were corrected with measurements of the field blank with the additional  
32 error from this correction propagated into our final reported values. The field blank chromatogram for the size-  
33 resolved BB samples is presented in Fig. S2.

## 34 **2.6 BC fire sample analysis**

35 The full method for the collection and extraction of BB particle samples collected during July wildfires in British  
36 Columbia is detailed in Di Lorenzo et al. (2016). Briefly, PM<sub>2.5</sub> samples were collected at two sites approximately

1 100 kilometers east of the biomass-burning location. The first site was located in Burnaby/Kensington Park (BKP)  
2 and the second was in North Vancouver/Second Narrows (NVSN). The particle samples were collected using real-  
3 time beta attenuation particle monitors (5030 SHARP Monitor at the BKP site, 5030i SHARP monitor at the  
4 NVSN site, Thermo Fisher Scientific, Waltham, MA, USA) at a  $16.67 \text{ L min}^{-1}$  flow rate in 8-hour intervals.  
5 Particles were collected on glass microfiber filter tape and stored at  $-20^\circ\text{C}$  until extracted. Approximately 37 %  
6 of each filter spot area was placed into a polypropylene vial with 10 ml of deionized water, and sonicated for 40  
7 minutes. The extracts were filtered with PTFE syringe filters (3 mm diameter,  $0.2 \mu\text{m}$  pore size, VWR  
8 International, Radnor, Pennsylvania, USA) and diluted by a factor of five with ultrapure deionized water [so that](#)  
9 [all analytes were in the calibration range](#) before being injected on the IC. [During the extraction, an unexposed area](#)  
10 [of the glass microfiber filter tape was sampled and extracted for use as a field blank. All calculated quantities and](#)  
11 [errors were blank-corrected using the field blank.](#)

12

### 13 3 Results and Discussion

#### 14 3.1 Analytical method performance of CS19 cation exchange column

##### 15 3.1.1 Separation approach and optimization of parameters

16 Our approach to separation involved injecting the highest mixed inorganic cation and mixed amine standards for  
17 the expected working range ( $0.1 - 2.5 \mu\text{g ml}^{-1}$ ) at static flow rates ( $0.75 \text{ ml min}^{-1}$ ,  $1 \text{ ml min}^{-1}$ , and  $1.25 \text{ ml min}^{-1}$ )  
18 while systematically increasing the isocratic eluent concentration (4 mM - 16 mM). The quality of each isocratic  
19 method was assessed by calculating the peak-to-peak resolution ( $R_s$ ) using the retention time ( $t_R$ ) and peak width  
20 at base (w) determined from the highest standard for each pair of cations following Eq. (1):

$$21 R_s = \frac{2(t_{R2} - t_{R1})}{w_2 + w_1}, \quad (1)$$

22 Using the upper limit of the expected working range for all analytes provides a lower limit on peak-to-peak  
23 resolution between these species. The peak-to-peak resolutions of the isocratic methods run using a  $0.75 \text{ ml min}^{-1}$   
24 and  $1.25 \text{ ml min}^{-1}$  flow rate for the selected inorganic and alkyl amine cations are presented in Fig. S3 and S4.  
25 Peak-to-peak resolution between all peaks increased as the mobile phase ionic strength was lowered when the flow  
26 rate was held constant. This is in agreement with Eq. (2), the fundamental resolution equation, which describes  
27 peak-to-peak resolution in terms of an efficiency factor (N), retention factor (k), and a selectivity factor ( $\alpha$ ).

$$28 R = \left(\frac{\sqrt{N}}{4}\right) \left(\frac{k}{k+1}\right) \left(\frac{\alpha-1}{\alpha}\right), \quad (2)$$

29 With low mobile phase ionic strength, the retention factor of the analytes is expected to increase, leading to greater  
30 resolution, consistent with our observations. In contrast, the effect of flow rate on peak resolution is non-intuitive  
31 and must be obtained empirically. Lower flow rates increase the retention factor, which in turn increases resolution.  
32 However, an increase in mobile phase flow rate has a competing effect on the efficiency factor in Eq. (2). The  
33 efficiency term is governed by the theoretical plate height (H) as described by the Van Deemter equation (Eq. (3)),  
34 which highlights the competing effect of flow rate ( $\mu$ ) on peak resolution:

1 
$$H = A + \frac{B}{\mu} + C\mu, \quad (3)$$

2 Figures S3 and S4 show no loss in peak resolution when using a higher flow rate (1.25 ml min<sup>-1</sup> vs 0.75 ml min<sup>-1</sup>). To confirm that there was no loss in efficiency at higher flows, Van Deemter plots were created, using MMAH<sup>+</sup> 3 and TEAH<sup>+</sup> as representative early and late-eluting species, by plotting theoretical plate height versus flow rate 4 (Fig. S5). To do this, the theoretical plate heights described in Eq. (3) were calculated using Eq. (4), which relates 5 H to column length (L), t<sub>R</sub> and w. The A, B and C terms of Eq. (3) were then determined by solving a system of 6 equations using the calculated H values for MMAH<sup>+</sup> and TEAH<sup>+</sup> at three isocratic flow rates as they are located 7 at opposite ends of the elution range of the six most abundant atmospheric alkyl amines (Fig. 1).

8 
$$\frac{L}{H} = 16 \left( \frac{t_R}{w} \right)^2, \quad (4)$$

9 The Van-Deemter plots for MMAH<sup>+</sup> and TEAH<sup>+</sup> show no sacrifice in resolution when operating at higher flow 10 rates and low eluent concentrations. The resolution between Mg<sup>2+</sup> and Ca<sup>2+</sup> as well as between TMAH<sup>+</sup> and TEAH<sup>+</sup> 11 improved at the higher flow rate for all isocratic eluent concentrations. This was due to a decrease in peak width 12 from diffusion band broadening. Furthermore, there was little to no sacrifice in resolution for all other cation peak 13 pairs when operating at a higher flow rate. Of particular note, utilizing a 4 mM MSA isocratic separation at a 1.25 14 ml min<sup>-1</sup> flow rate instead of a 0.75 ml min<sup>-1</sup> flow resulted in a runtime that was 20 minutes shorter, which improves 15 the applicability of IC for near-real-time analysis of hourly to bi-hourly atmospheric sample collection timescales. 16 A shorter run time also improves the method throughput capacity for offline analyses and reduces total eluent 17 consumption. For these reasons, the faster flow rate was selected in designing and optimizing a gradient program. 18 Further isocratic methods using lower MSA concentrations (1 mM and 2 mM) were run at a 1.25 ml min<sup>-1</sup> flow 19 rate to quantify values of peak-to-peak resolution for the inorganic cations and alkyl amines before approaching a 20 gradient method (Fig. S3 and S4). An increase in resolution greater than one was observed for all analyte pairs 21 aside from DEAH<sup>+</sup>/TMAH<sup>+</sup> when using a 1 mM MSA eluent concentration.

22 All gradient methods that were tested started with a 1 mM hold, followed by a step-wise increase and/or ramp to 23 higher eluent concentrations at a column temperature of 30 °C. By combining the best isocratic separations for 24 various pairs of cation analytes sequentially, iterative modifications were used to improve resolution based on Eq. 25 (1-3) with the best separation method selected from amongst the iterations. [Higher column temperature has been](#) 26 [used to improve the quality of a separation method \(Hatsis and Lucy, 2001; van Pinxteren et al., 2015; Rey and](#) 27 [Pohl, 1996; Rey and Pohl, 2003\)](#). Therefore, column temperature was systematically increased to investigate if 28 further improvement in peak-to-peak resolution was possible. Temperature effects on separation efficiency in ion 29 chromatography are thermodynamically complex (Hatsis and Lucy, 2001; Kulic, K., 2004; Rey and Pohl, 1996), 30 but typically result in increased peak resolution because of improvements in mobile phase diffusivity, which 31 increases the efficiency term from Eq. (2). Higher temperatures can replicate the separation effects observed when 32 adding an organic mobile phase modifier (Hatsis and Lucy, 2001; Rey and Pohl, 1996). Figures 1a and b show 33 gradient separations at 30 °C and 55 °C respectively. At 30 °C, K<sup>+</sup> and DMAH<sup>+</sup> overlap considerably (R<sub>S</sub> = 0.45) 34 and DEAH<sup>+</sup> and TMAH<sup>+</sup> coelute. By increasing the column temperature to 55 °C, the extent of peak overlap 35 between K<sup>+</sup> and neighboring alkyl amine cations is noticeably reduced (R<sub>S</sub> > 1) and DEAH<sup>+</sup> and TMAH<sup>+</sup> are 36 increasingly well resolved (R<sub>S</sub> = 1.48). The effect of temperature on the separation of the alkyl amines is 37

1 demonstrated in Fig. 2, where the separation of  $\text{DEAH}^+$  with  $\text{TMAH}^+$  is achieved above 50 °C. The temperature  
2 increase also results in lower resolution between  $\text{DMAH}^+$  and  $\text{MEA}^+$  from  $R_S = 1.57$  to  $R_S = 1.08$ . In our method,  
3 a column temperature of 55 °C produced peak-to-peak resolutions greater than a value of one between all six alkyl  
4 amine cations and inorganic cations in the final gradient method, giving a 95 % separation between our target  
5 analytes and expected atmospheric interferences in the condensed phase. The peak-to-peak resolutions are  
6 summarized in Table 1. These represent a lower-limit in peak resolution since they were calculated using peak  
7 parameters at the upper limit of the working range, which was determined based on maximum mixing ratios or  
8 mass loadings expected for the analysis of atmospheric samples containing these analytes.

9 The separation method produced in this work is able to overcome previously reported IC coelution difficulties  
10 between  $\text{DEAH}^+$  and  $\text{TMAH}^+$  and between  $\text{MEA}^+$  and  $\text{DMAH}^+$  (VandenBoer et al., 2012; Verriele et al., 2011).  
11 Both DMA and TMA have been identified as dominant amines in emission studies, so it is important to achieve  
12 accurate and specific quantitation of both species in gas and particulate atmospheric samples (Facchini et al., 2008;  
13 Kuwata et al., 1983; Müller et al., 2009; Van Neste and Duce, 1987). Multiple field campaigns have detected large  
14 quantities of [gas-phase and particle-phase](#) MEA and DEA in ambient air as well (Facchini et al., 2008; Müller et  
15 al., 2009; Sorooshian et al., 2009; Yang et al., 2005; Yang et al., 2004). In some cases clean up steps have been  
16 used to alleviate IC interferences from common atmospheric cation species in the quantitation of amines despite  
17 the fact that an 85% evaporation loss of the amines, in addition to the extra sample handling, was reported when  
18 using a solid phase extraction clean up (Huang et al., 2014). The CS19 IC method reported here is able to separate  
19 the most common atmospheric inorganic cations in addition to eleven common atmospheric amines (see additional  
20 separation of five additional alkyl amines in Sect 3.1.3). It can be easily applied to water-soluble atmospheric gas  
21 and particulate samples since they can be directly analyzed - without coelution or a clean-up step - with separation  
22 times of similar duration to many previously reported methods, including those employing an online IC method  
23 (Huang et al., 2014; Murphy et al., 2007; VandenBoer et al., 2012; Verriele et al., 2011).

24 **3.1.2 Instrumental performance and comparison for the methyl amines, ethyl amines and inorganic  
25 cations**

26 The performance statistics of the CS19 gradient method for each cation are summarized in Table 1. The method  
27 shows high reproducibility, with method precisions better than 10 % for most analytes. [Although the instrumental  
28 response varied from month-to-month for each analyte, this variability was random and the calibration curve slopes  
29 for each analyte showed no systematic decrease over time](#). The larger variability in the  $\text{TMAH}^+$  and  $\text{TEAH}^+$   
30 calibration curves ( $\pm 16\%$  and  $\pm 11\%$  respectively) is likely driven by their lower Henry's Law constants ( $K_H$ ) in  
31 water (Christie and Crisp, 1967), resulting in volatilization losses from standards. Concurrently, this variability  
32 could be driven by partitioning losses along the flow path, particularly when the tri-substituted amines reach the  
33 suppressor, which was not temperature-controlled. In future investigations it may be worthwhile to acidify the  
34 standards to ensure the amines are maintained in their charged form in the aqueous phase. Alternatively, to combat  
35 losses to neutral forms, use of a Salt Converter suppressor accessory (ThermoScientific, SC-CSRS 300, P/N:  
36 067530), which keeps weak electrolytes in a separated sample fully protonated prior to their conductance  
37 measurement, may also aid in increasing long-term  $\text{TMAH}^+$  and  $\text{TEAH}^+$  precision.

1 The limits of detection (LODs) for each analyte are reported in Table 1 as both a range and as the average LOD  
2 ( $\pm 1\sigma$ ). The LODs are reported in this manner to reflect the high day-to-day variability in the calculated LODs.  
3 This variability may be driven by i) the purity of the deionized water used for eluent generation; ii) instrumental  
4 baseline noise and trace contamination on the day of analysis; and iii) quality of labware cleaning prior to  
5 preparation of calibration blanks. Outliers in the LOD dataset were found to result from trace contamination of  
6 analytical labware, sampling vials, or from systematic errors made in the preparation of standards or injection of  
7 samples on the IC (e.g. leaking autosampler caps, failing retention of concentrator column). The Grubb's test was  
8 performed using a 95% confidence interval to statistically identify outliers from LOD data sets. Calculated  
9 detection limits were determined to lie in the picogram per injection range for all analytes. The LODs for the  
10 inorganic cations were 10 to 100 times lower than those of the alkyl amines, with the exception of  $Mg^{2+}$  and  $Ca^{2+}$ .  
11 Trace contamination of calcium in our ultrapure deionized water led to higher LODs for the divalent cations. Our  
12 method shows high accuracy in the upper range of the calibrations for the methyl and ethyl amines, with accuracies  
13 ranging from 90 – 100 %. The accuracy was much lower for each methyl and ethyl amine cation at the low end of  
14 the calibration range where amine concentrations were approximately 1.5 times the limit of quantitation (LOQ).  
15 Quantitation near the method LOQ was more sensitive to small integration changes, which affected the calculated  
16 peak area, even when performing integrations manually, and this resulted in greater method error. This is a  
17 drawback inherent to IC since wide analyte peaks are a result of persistently large stationary phase particle sizes,  
18 causing band broadening via longer flow paths and increased diffusion during separation (i.e. the A and B terms  
19 in Eq. (3)). The low alkyl amine accuracies may also be driven by their air-water partitioning properties, which  
20 could result in losses during sample handling and during sample injection. The low and high range accuracies for  
21 all inorganic cations, with the exception of ammonium, were high (80 – 120%) because concentrations were not  
22 near the limit of quantitation for these analytes. The low check standard accuracy for ammonium likely arises due  
23 to similar issues as those discussed above for the tri-substituted amines.

24 To further test the efficacy of the separation method, a standard addition calibration was performed in the presence  
25 of the complex BB matrix. The calibration slopes and retention times for each analyte from the standard addition  
26 and external calibration performed on the same day are listed in Table S1. The slopes for the two calibrations  
27 varied between 0 and 8 %, which is within the method calibration precisions presented in Table 1. Thus, the BB  
28 sample extracts did not exhibit matrix effects as the slopes were found to be within the expected instrument  
29 variability as determined by external calibration standard analysis. However, increasing retention times of  
30 approximately 0.3 – 0.5 minutes were observed for all cation analytes when performing the standard addition. This  
31 is an effect inherent in IC when samples with higher total quantities of cations are preconcentrated, resulting in a  
32 sample plug filling a greater volume of the stationary phase capacity. The initial weak mobile phase of the gradient  
33 method will therefore take a greater amount of time to elute all of the analyte cations from the preconcentration  
34 and analytical columns. This same increase in retention times is present in the external calibration with increasingly  
35 concentrated standards (Table 1).

36 Previous IC instrumental precisions reported for use in quantifying the six atmospheric methyl and ethyl amines  
37 range from 0.4 to 17.2 %, which are comparable to our method (Table S2; Chang et al., 2003; Dawson et al., 2014;  
38 Erupe et al., 2010; Huang et al., 2014; Li et al., 2009; VandenBoer et al., 2012; Verriele et al., 2012;). Our  
39 separation method shows greater average variability than others due to our numerous assessments ( $n = 9$ ) over

1 multiple months, a more comprehensive analysis compared to previous reports. The sensitivity of this instrument  
2 is also similar to that of all other reported IC methods as the instrumental detection limits are in the picogram  
3 range. Only VandenBoer et al. (2012) and Chang et al. (2003) report lower detection limits and these are likely a  
4 result of a lower background signal from running the IC instruments online. Our method does not achieve  
5 instrumental limits of detection as low as those achieved using derivatization methods coupled with GC-MS or  
6 HPLC analysis (Akyüz, 2007; Fournier et al., 2008; Possanzini and Di Palo, 1990). However, multi-step  
7 derivatization methods are prone to losses that must be quantified with internal standards. These losses can lead  
8 to higher overall method detection limits, which is not the case for direct analysis of water-soluble samples.  
9 Derivatization methods are also difficult to employ for near-real-time analyses of the atmosphere, making the  
10 approach less analytically attractive. Further, the IC separation method presented here is able to address additional  
11 matrix effects that may result from other atmospheric species through the use of a sample pre-concentration  
12 column. Only positively charged species are retained in this pre-concentration step and injected through the IC  
13 system for analysis, negating matrix effects from non-charged and anion species, as demonstrated by the standard  
14 addition to the BB sample extract.

15 Employing a method that is capable of quantifying amines at very low mixing ratios is valuable since recent work  
16 has shown that [parts per quadrillion by volume \(ppqv\)](#) concentrations of gaseous amines can lead to particle  
17 formation and growth (Almeida et al., 2013). If our method were applied to online atmospheric ambient sampling  
18 of gases or particles the method could be used to detect amines at [ppqv](#) mixing ratios. For example, a detectable  
19 signal for 100 ppqv mixing ratios could be attained by sampling through a bubbler, filter, or denuder at a low flow  
20 rate of  $3 \text{ L min}^{-1}$  for 1 – 10 hours, depending on the amine. It may be possible to shorten the sample collection  
21 duration to an hourly timescale to detect [ppqv](#) mixing ratios of atmospheric amines if the method is interfaced with  
22 a high sensitivity MS detector. Verriele et al. (2014) observed a 5 – 30 fold improvement in method detection  
23 limits when interfacing their IC method with a MS detector.

### 24 **3.1.3 Expanded amine catalogue for other common atmospheric species**

25 The separation method developed was further investigated to elucidate its utility in quantifying monopropylamine  
26 (MPA), isomonopropylamine (iMPA) and monobutylamine (MBA), three additional amines that have been  
27 frequently detected in ambient air (Ge et al., 2011). In particular, this test was performed to assess their potential  
28 coelution with the fully separated methyl and ethyl amines. Without modification of the gradient method, we  
29 observed separation of these three additional amines from the original twelve cations with  $R_s \geq 0.85$  (Fig. 3a).  
30 MPAH $^+$  and iMPAH $^+$  eluted between DMAH $^+$  and TMAH $^+$  and MBAH $^+$  eluted later, but before TEAH $^+$ . The  
31 resolution is sufficient between all analyte peaks to allow quantitative analysis of the nine alkyl amine cations and  
32 six inorganic cations. The separation statistics for these additional amines are also presented in Table 1. Since the  
33 additional amines were injected after column degradation had occurred and retention times had noticeably shifted  
34 (see Fig. 3a vs. Fig. 1b [and Sect 3.1.5 for further discussion](#)), retention time and peak width were estimated using  
35 changes in separation parameters from the original method development for the methyl and ethyl amines. Peak  
36 widths for the propyl and butyl amines were assumed to have increased by approximately 50 %, consistent for the  
37 same increases observed for the methyl and ethyl amines as a result of the column degradation. Retention times  
38 for MPAH $^+$ , iMPAH $^+$ , and MBAH $^+$  were back-calculated to reflect the initial column conditions using these

1 corrected peak widths and the resolution values determined from the chromatogram presented in Fig. 3. The  
2 method precisions for iMPAH<sup>+</sup>, MPAH<sup>+</sup> and MBAH<sup>+</sup> determined from two standard calibration injections ranged  
3 from 1 - 12 %. The reported average LODs for both propyl amines are the lowest of the alkyl amines, while  
4 MBAH<sup>+</sup> has the highest method LOD because it elutes in a region with a high background due to the step change  
5 in eluent composition not being completely suppressed. The method accuracies for the three additional amines  
6 assessed by both the high and low check standards were within 80 % for all analytes. However, the large standard  
7 deviations in the accuracies for all low check standards highlights the challenge of method reproducibility for these  
8 analytes near the limit of quantitation. This CS19 IC method can resolve three sets of alkyl amine structural  
9 isomers, therefore not only allowing full speciation of the suite of common atmospheric amines, but also  
10 overcoming a limitation of direct mass spectrometry analysis of the atmospheric matrix.

11 Since diamines have recently been shown to be potent sources of new particle formation and have been detected  
12 in field campaigns across the U.S.A. (Jen et al., 2016b), as well as near livestock, food processing factories and  
13 sewage facilities (Ge et al., 2011), quantitation of 1, 4-diaminobutane (DABH<sup>+</sup>) and 1, 5-diaminopentane (DAPH<sup>+</sup>)  
14 was tested using the CS19 gradient method. The two diamines eluted after all 15 analytes, with DABH<sup>+</sup> and Ca<sup>2+</sup>  
15 having a peak-to-peak resolution of 3.16 and DAPH<sup>+</sup> and DABH<sup>+</sup> having a peak-to-peak resolution of 0.98. A  
16 single calibration curve was run to provide an estimate of the sensitivity and LOD for DABH<sup>+</sup> and DAPH<sup>+</sup> and  
17 the retention times for these two additional diamines were also back-calculated to reflect initial column conditions  
18 (Table 1). If the 10 mM MSA hold of the optimized method is extended by 5 minutes to give a total run time of  
19 40 minutes, then DABH<sup>+</sup> and DAPH<sup>+</sup> can also be quantified. Ethanolamine (EAH<sup>+</sup>), a compound employed in  
20 industry and CO<sub>2</sub> capture (Ge et al., 2011), was also analyzed by this IC method and found to have poor resolution  
21 with NH<sub>4</sub><sup>+</sup> and MMAH<sup>+</sup> ( $R_s \leq 0.65$ , Table 1). However, the peak is still identifiable in samples containing these  
22 analytes.

### 23 **3.1.4 Method development with the addition of an inline CG15 guard column**

24 As mentioned previously, IC methods in the literature have been unable to separate potassium from the methyl  
25 and ethyl amines (Huang et al., 2014; VandenBoer et al., 2012), and in our current method potassium has slight  
26 overlap with MMAH<sup>+</sup> ( $R_s = 1.09$ ). We attempted to reduce peak overlap between potassium and the alkyl amines  
27 by adding a crown ether-functionalized CG15 guard column in-line after the CG19/CS19 columns. The addition  
28 of the CG15 column, which has increased selectivity for K<sup>+</sup>, resulted in an increased retention time for potassium  
29 of 13 minutes. The best separation achieved using the additional guard column is shown in Fig. 3b, where K<sup>+</sup> still  
30 elutes within the alkyl amine retention region. The gradient method used to achieve the separation used a flow rate  
31 of 1 ml min<sup>-1</sup>, a column temperature of 55 °C, and held a 1 mM MSA concentration for the first 30 minutes. The  
32 eluent concentration was step increased to 4 mM followed immediately by an exponential ramp to 10 mM over 20  
33 minutes (Chromeleon curve factor = 7). The final concentration of 10 mM is held for an additional 15 minutes,  
34 yielding a total run time of 65 minutes. Even when holding the initial MSA concentration at 1 mM for 50 minutes,  
35 the separation was unable to fully resolve the alkyl amine peaks. An increase in retentivity for K<sup>+</sup> and NH<sub>4</sub><sup>+</sup> as  
36 well as many of the alkyl amines, indicated that the crown ether functionality was not selective for K<sup>+</sup> in this suite  
37 of analytes. With the addition of an organic modifier to the mobile phase or the ability to decrease column  
38 temperature, this increase in selectivity from the CG15 column might be harnessed to produce better separation.

1 However, due to the limitations of the ICS-2100 system using RFIC we were unable to investigate these  
2 parameters. Furthermore, although a passable separation may be achieved when using a run time greater than 60  
3 minutes, this would not be as applicable to online analyses as the CG/CS19 method developed without the addition  
4 of the CG15 column. A stationary phase similar to that of the CG/CS19 columns, but with some of this crown  
5 ether selectivity could potentially yield better results than those presented here, particularly for the analysis of  
6 atmospheric samples containing large quantities of  $K^+$  and amines.

7 **3.1.5 Analytical column stability**

8 Over the course of five months, peak retention times noticeably decreased and peak broadening of approximately  
9 50 % occurred for all analytes. After more than 1000 sample and standard injections retention times had decreased  
10 by  $1.9 \pm 0.1$  minutes depending on the cation. Peak-to-peak resolution, however, remained largely unchanged  
11 throughout the column degradation during standard and sample analysis, even with observed peak broadening.  
12 This is consistent with what has been previously reported in the literature when hundreds to thousands of injections  
13 have been run through an IC column (VandenBoer et al., 2011). This may also be a result of column degradation  
14 from operating the CS19 column at a temperature higher than that recommended by the manufacturers.

15 During the course of method development severe peak broadening and subsequent peak-to-peak resolution loss of  
16 magnesium and calcium was also observed. After the analysis of hundreds of samples the unresolved co-eluting  
17 divalent cations had a peak width greater than 10 minutes wide. The magnesium and calcium peak areas eventually  
18 became unresolved, with their combined peak area precision in the highest standard within 6 % ( $\pm 1\sigma$ ) after 12  
19 months of analysis. It was determined that this broadening effect observed for the  $Mg^{2+}$  and  $Ca^{2+}$  peaks was due  
20 to a malfunctioning suppressor. After replacing the suppressor, a peak-to-peak resolution greater than one was  
21 restored for these analytes. Furthermore, the cumulative analyte peak broadening that had occurred throughout  
22 method development and sample analysis for all the monovalent cations was also mitigated by installing the new  
23 suppressor. Retention times however were still shifted by  $1.9 \pm 0.1$  minutes, indicating that analytical column  
24 degradation had still occurred.

25 **3.2 Biomass-burning particle analysis and discussion**

26 **3.2.1 Size-resolved alkyl amines in particles from an aged biomass-burning plume**

27 Biomass-burning particles often contain a complex mixture of water-soluble ions, organics, elemental carbon and  
28 other insoluble components, making them nonpareil for testing the robustness of an atmospheric measurement  
29 technique. Ions such as  $NH_4^+$  and  $K^+$  are consistently detected in biomass burning plumes, regardless of sampling  
30 location as they are well characterized as being co-emitted species (Capes et al., 2008; Hudson et al., 2004; Pósfai  
31 et al., 2003). Particles released during forest fires have also been shown to contain highly oxidized large molecular  
32 weight organics (Di Lorenzo and Young, 2016; Saleh et al., 2014). We tested the robustness of our method on  
33 water-extracted aged biomass-burning particle samples collected by a cascade impactor in St. John's, Canada.  
34 Gas-sorption and reaction artifacts are minimized due to the gaseous flow-path being directed around the  
35 nanoMOUDI impaction plates, therefore samples analyzed are representative of the particles in the atmosphere.  
36 An overlaid chromatogram of two different size-resolved particle samples (100 - 180 nm and 320 – 560 nm) shows

1 the presence of  $\text{MMAH}^+$ ,  $\text{DMAH}^+$  and  $\text{DEAH}^+$  in the aged biomass burning samples with complete separation  
2 from  $\text{K}^+$ ,  $\text{NH}_4^+$  and  $\text{Na}^+$  (Fig. 4). The maximum mass loadings for  $\text{MMAH}^+$ ,  $\text{DMAH}^+$  and  $\text{DEAH}^+$  were found in  
3 particles with diameters ( $D_p$ )  $320 - 560$  nm and were  $11 \pm 3$   $\text{ng m}^{-3}$ ,  $208 \pm 4$   $\text{ng m}^{-3}$ ,  $1300 \pm 200$   $\text{ng m}^{-3}$ , respectively  
4 (Table S3).  $\text{TMAH}^+$ ,  $\text{MEAH}^+$  and  $\text{TEAH}^+$  peaks were also detected in the BB size-resolved particle extracts.  
5  $\text{TMAH}^+$  and  $\text{TEAH}^+$  reached mass loadings of  $5 \pm 3$   $\text{ng m}^{-2}$  and  $4 \pm 2$   $\text{ng m}^{-3}$ , respectively, while  $\text{MEAH}^+$  never  
6 exceeded a concentration of  $1$   $\text{ng m}^{-3}$  in any size-resolved particle fraction (Table S3). The relative loadings of  
7  $\text{NH}_4^+$ ,  $\text{K}^+$  or  $\text{Na}^+$  to individual amines in these samples ranged from 2:1 to 1000:1, demonstrating the robustness  
8 of this method to quantify amines. Lobert et al (1990) reported detecting  $\text{C}_1 - \text{C}_5$  aliphatic amines from controlled  
9 biomass-burning experiments, which is consistent with our findings. BB-derived amines were also identified  
10 during the 2007 San Diego forest fires (Zauscher et al., 2013) with primary amines observed at approximately 6%  
11 by mass of organic content from an aged biomass burning particle sample in British Columbia (Takahama et al.,  
12 2011). However, few studies have addressed the speciation and quantitation of alkyl amines emitted from biomass-  
13 burning events. Schade and Crutzen (1995) estimated the emission rates for MMA, DMA, TMA and MEA from  
14 biomass burning sources based on controlled burn experiments, but do not include a BB emission rate for DEA or  
15 TEA. These emission inventories are yet to include emission rates from atmospheric BB measurements (Lobert et  
16 al., 1990; Schade and Crutzen, 1995).

17 In Figure 5a we show the molar ratio of the sum of the methyl and ethyl amines to ammonia which is considered  
18 to be the main atmospheric base, as a function of the size-resolved particles collected. The summed amine moles  
19 exceeded ammonium [in the particle diameter range](#) from 100 to 560 nm, and the ratio ranged from 0.5 to 1.9 in  
20 the fine mode ( $\text{PM}_{1.0}$ ), with an average ratio of 0.92 in  $\text{PM}_{1.0}$  calculated using nanoMOUDI bins up to this nominal  
21 cutoff. Quantities of  $\text{NH}_4^+$  were below the detection limit in samples above  $1 \mu\text{m}$ , yielding no values for the ratio.  
22 The large error bars in the ratios are driven by the low molar quantities of ammonium in the samples as well as a  
23 higher than normal variability in three extraction blanks (ultrapure deionized water in polypropylene tubes)  
24 injected on the day of analysis. For these reasons this method blank error was assigned to the size-resolved samples  
25 in place of the  $\text{NH}_4^+$  error driven by the method precision and accuracy detailed in Table 1. To our knowledge,  
26 this is the first time that an amines to ammonium ratio greater than one has been reported in the  $\text{PM}_{1.0}$  resolved  
27 fraction of atmospheric particles. An amines to ammonium ratio of 0.37 in fine mode aerosol ( $\text{PM}_{1.8}$ ) was reported  
28 by VandenBoer et al. (2011), but most reported ratios have been below 0.1 (Ge et al., 2011). The high ratios we  
29 observed can be attributed to large quantities of  $\text{DEAH}^+$  and  $\text{DMAH}^+$ .  $\text{MMAH}^+$  was found to be in molar quantities  
30 100 times less than that of ammonium while  $\text{TMAH}^+$ ,  $\text{MEAH}^+$  and  $\text{TEAH}^+$  were found to be in molar quantities  
31 1000 to 10000 times less than ammonium. Detecting such large molar ratio quantities of  $\text{DEAH}^+$  and  $\text{DMAH}^+$  to  
32  $\text{NH}_4^+$  in any particle sample is also unprecedented. Mono-substituted amines are the most frequently detected alkyl  
33 amines in atmospheric particles and at molar ratios to ammonium of 1:100 or lower (Ge et al., 2011; Gorzelska et  
34 al., 1990; Mader, 2004, Müller et al., 2009; Yang et al., 2005; Yang et al., 2004; Zhang et al., 2003). In most  
35 instances where di-substituted or tri-substituted amines have been identified in the particle phase, they are present  
36 at molar quantities equal to or less than the mono-substituted amines (Healy et al., 2015; Suzuki et al., 2001). Thus,  
37 such high quantities of  $\text{DMAH}^+$  and  $\text{DEAH}^+$  in these samples were unexpected and highly unusual compared to  
38 prior reports. In this case, the observation may be due to the fuel source of the fire or the interaction of the plume  
39 with a potent source of atmospheric amines. Previous work has identified di-substituted amines in large quantities

1 from feedlot plumes (Sorooshian et al., 2008) and in marine particles (Facchini et al., 2008; Gibb et al., 1999a;  
2 Müller et al., 2009; Sorooshian et al., 2009; [Van Pinxteren et al., 2015](#); Youn et al, 2015). In fact, DMA and DEA  
3 have been reported as the second- and third-most abundant organic species in marine fine aerosol behind  
4 methanesulfonic acid during periods of high biological activity in the North Atlantic (Facchini et al., 2008). Other  
5 researchers have also suggested a moderate to high correlation between high biological activity and di-substituted  
6 amine particle mass loadings (Müller et al., 2009; Sorooshian et al., 2009). Laboratory investigations have shown  
7 that methylamines can be produced by marine phytoplankton degradation of quaternary amines to maintain an  
8 osmotic gradient as well as during periods of known zooplankton grazing (Gibb et al., 1999b). Based on the  
9 HYSPLIT back-trajectories calculated for these samples (Di Lorenzo, 2016), it is possible that the BB plume  
10 particles interacted with gaseous DMA and DEA emitted from inland agricultural sources along the St. Lawrence  
11 River, coastal phytoplankton blooms, or with enhanced amine emissions in the coastal zone, which has been  
12 observed in the marine boundary layer of California (Youn et al., 2015). The high concentrations of DMA and  
13 DEA produced by marine biological activity could then partition into the biomass burning particles and react to  
14 neutralize inorganic acids (e.g. sulfuric acid), form salts or amides with organic acids, or react with carbonyl  
15 moieties in the highly oxidized organic material produced via BB to form imines (Qiu and Zhang, 2013). [If this explanation holds true then there may be preferential uptake of these amines over ammonia into the plume, as there is no evidence yet that suggests a larger agricultural or marine source of amines relative to ammonia to the atmosphere.](#) In particular, a marine amines hypothesis, while consistent with observations in the literature, is  
16 beyond the scope of this work in terms of assigning a definitive DMA and DEA source.  
17  
18

### 20 **3.2.2 Time series of amines in fresh biomass burning plume particles from British Columbia**

21 Our method was also applied to a time series of PM<sub>2.5</sub> samples collected at two different locations (BKP and  
22 NVSN) during a forest fire in the Lower Fraser Valley in British Columbia in the summer of 2015. These PM<sub>2.5</sub>  
23 samples were collected every 8 hours while the plume was traversing each site and [during collection](#) the PM<sub>2.5</sub>  
24 concentration was in excess of 200  $\mu\text{g m}^{-3}$ . The relative ages for the smoke plumes sampled at both sites were  
25 calculated to be 20 hours old, or less, and back trajectories indicated that the plume did not travel over the open  
26 ocean before being sampled (Di Lorenzo et al., 2016). In these test samples, the method was again able to detect  
27 the presence of four different amines (iMPAH<sup>+</sup>, TMAH<sup>+</sup>, DEA<sup>+</sup>, and TEAH<sup>+</sup>) with loadings of Na<sup>+</sup>, NH<sub>4</sub><sup>+</sup> and  
28 K<sup>+</sup> at ratios in excess of 100:1 (Figure S6). Furthermore, the method was not only able to determine the presence  
29 of isomonopropylamine, but also differentiate it from monopropylamine and trimethylamine, its two structural  
30 isomers. iMPAH<sup>+</sup>, TMAH<sup>+</sup>, DEA<sup>+</sup>, and TEAH<sup>+</sup> had maximum mass loadings in these fresher biomass-burning  
31 samples of  $60 \pm 40 \text{ ng m}^{-3}$ ,  $9 \pm 7 \text{ ng m}^{-3}$ ,  $1.6 \pm 0.8 \text{ ng m}^{-3}$ , and  $0.2 \pm 0.1 \text{ ng m}^{-3}$  respectively (Table S4). iMPAH<sup>+</sup>  
32 was the amine detected in the largest molar quantities at both sampling sites in British Columbia. The detection of  
33 iMPAH<sup>+</sup> has not previously been reported in biomass-burning emission inventories, and based on our  
34 measurements may be important to quantify in future controlled burn experiments. Our results differ from the  
35 study conducted by Takahama et al (2011) on the 2009 forest fires in British Columbia that reports the detection  
36 of primary amine groups, which further suggest that amine emissions from biomass burning and/or their  
37 incorporation into biomass burning particles are not well understood. Although our observed suite of amines  
38 includes iMPAH<sup>+</sup>, there was no indication of other primary amines from the analyses of the BB particles. [The calculated quantities for these samples may be biased high or low because the beta attenuation monitor used to](#)  
39

1 sample the BB particles can be prone to gas-phase blow-on or blow-off artifacts via sorption or reactive  
2 mechanisms, as per traditional filter sampling strategies. Although the extracted field blank was corrected for any  
3 positive sorption biases on the filter tape (e.g. Müller et al., 2009), it was unable to account for any reactive uptake  
4 of gas-phase amines during the sampling period. Therefore, the filter tape BB samples presented here represent a  
5 time-integrated particulate composition assuming thermodynamic equilibrium between the gas and particulate  
6 phases for the duration of collection for each sample.

7 A time-series of the amines to ammonium molar ratio as the smoke plume intrudes into both the BKP and NVSN  
8 sites is presented in Fig. 5b. There were either no amines present or they were present in concentrations below our  
9 detection limits in the ambient particles collected on the front edge of the plume intrusions. When the maximum  
10 PM<sub>2.5</sub> mass loading of the plume reached the sampling site at t = 0, we saw an absolute maxima in total amine  
11 concentration as well as a relative maxima in the particulate amine to ammonia molar ratio (Fig. 5b). The  
12 particulate amine concentrations and the amines to ammonia ratio then tapered off as the plume diluted and passed  
13 through the site. The measured amines to ammonia ratio in these samples is consistent with previously reported  
14 literature values (Ge et al., 2011). The measured amine species and quantities, as in the aged plume, could be  
15 indicative of the biomass-burning source fuel, fire type, or amine levels in air masses intercepted that were  
16 subsequently incorporated by partitioning and reacting into the condensed phase. Since the smoke plumes were  
17 less than a day old and the plume did not travel over the open ocean, it is less likely that offshore marine amine  
18 emissions interacted with the plume. However, the BKP and NVSN sampling sites are positioned in a coastal  
19 urban center and anthropogenic amine emissions from industry or animal husbandry operations nearby, as well as  
20 coastal amine emissions, may still have been incorporated into the plume before it was sampled.

#### 21 4. Conclusions

22 We developed an ion chromatographic method that can separate and quantify nine dominant atmospheric alkyl  
23 amines and two alkyl diamines from common inorganic atmospheric cations. Ion chromatography methods  
24 reported in the literature cannot fully resolve alkyl amine peaks, nor separate interferences from potassium,  
25 magnesium and calcium. In this work, we report the ability to overcome these prevalent issues for atmospheric  
26 sampling with a rapidity that can also be applied to near real-time analyses of aqueous atmospheric extracts by IC.  
27 Additionally, the method is able to separate and quantify three pairs of structural isomers, a limitation for direct  
28 particle and gas sampling mass spectrometry instrumentation in quantifying atmospheric alkyl amines. The method  
29 detection limits are comparable to other published IC methods in the literature, however the described method is  
30 not as sensitive as instrumentation used in conjunction with derivatization methods coupled with GC-MS or LC-  
31 MS, which can suffer from sample processing losses.

32 The IC method is robust. Two sets of BB particle samples collected at two different locations in Canada were  
33 injected onto the IC column and the method detected and quantified amines in the presence of a complex matrix  
34 where inorganic analytes, such as K<sup>+</sup>, reached ratios of 1000:1 relative to the alkyl amines. A standard addition  
35 demonstrated that the BB matrix does not have any influence on the ability of the IC method to quantify these  
36 analytes. This is a major improvement over all prior reports of the application of IC to the detection of amines in  
37 aqueous extracts of atmospheric particulate matter. Our results suggest that increasing focus on speciation and

1 quantitation of various alkyl amines from direct BB emissions and their propensity to undergo reactive uptake with  
2 biomass burning particles are needed to constrain global budgets of atmospheric sources and fate of alkyl amines.  
3 Overall, the developed IC method shows promise for i) adoption into standard analysis of water soluble  
4 atmospheric extracts; ii) incorporation into online instrumentation already using ion chromatography for near real-  
5 time analysis of water soluble atmospheric samples; and iii) interfacing with high-resolution mass spectrometry  
6 for even higher analytical sensitivity, particularly where supporting measurements for ppqv-levels of amines may  
7 be stimulating new particle formation in the atmosphere.

8 *Author contribution.*

9 TCV designed the experiments and BKP, ATQ, and RAD carried them out. BKP prepared the manuscript with  
10 contributions from all co-authors.

11 *Competing interests.*

12 The authors declare that they have no conflict of interest

13 *Acknowledgements.*

14 The authors thank Geoff Doerksen at the Lower Fraser Valley Air Quality Monitoring Network in British  
15 Columbia for supplying biomass burning samples. Thanks to Joseph Bautista for help collecting biomass burning  
16 samples in St. John's, as well as Jamie Warren and Kathryn Dawe for their assistance in method development.  
17 Finally, the authors would like to thank Dr. Cora Young for her helpful comments in the writing of the manuscript.  
18 TCV was supported by a Government of Canada Banting Postdoctoral Fellowship and the ICS-2100 was procured  
19 through the Canadian Foundation for Innovation. Funding for this work was provided by the Government of  
20 Newfoundland and Labrador Department of Forestry and Agrifoods through a Centre for Forestry Science and  
21 Innovation grant (Project No. 221269).

22

23

24

25

1 References

2

3 Aiken, A. C., Salcedo, D., Cubison, M. J., Huffman, J. a., DeCarlo, P. F., Ulbrich, I. M., Docherty, K. S., Sueper, D., Kimmel, J. R., Worsnop, D. R., Trimborn, a., Northway, M., Stone, E. a., Schauer, J. J., Volkamer, R., Fortner, E., de Foy, B., Wang, J., Laskin, a., Shutthanandan, V., Zheng, J., Zhang, R., Gaffney, J., Marley, N. a., Paredes-Miranda, G., Arnott, W. P., Molina, L. T., Sosa, G. and Jimenez, J. L.: Mexico City aerosol analysis during MILAGRO using high resolution aerosol mass spectrometry at the urban supersite (T0) – Part 1: Fine particle composition and organic source apportionment, *Atmos. Chem. Phys.*, 9, 6633–6653, doi:10.5194/acpd-9-8377-2009, 2009.

4

5

6

7

8

9

10 Akyüz, M.: Simultaneous determination of aliphatic and aromatic amines in indoor and outdoor air samples by gas chromatography-mass spectrometry, *Talanta*, 71(1), 486–492, doi:10.1016/j.talanta.2006.10.028, 2007.

11

12

13

14 Almeida, J., Schobesberger, S., Kürten, A., Ortega, I. K., Kupiainen-Määttä, O., Praplan, A. P., Adamov, A., Amorim, A., Bianchi, F., Breitenlechner, M., David, A., Dommen, J., Donahue, N. M., Downard, A., Dunne, E., Duplissy, J., Ehrhart, S., Flagan, R. C., Franchin, A., Guida, R., Hakala, J., Hansel, A., Heinritzi, M., Henschel, H., Jokinen, T., Junninen, H., Kajos, M., Kangasluoma, J., Keskinen, H., Kupc, A., Kurtén, T., Kvashin, A. N., Laaksonen, A., Lehtipalo, K., Leiminger, M., Leppä, J., Loukonen, V., Makhmutov, V., Mathot, S., McGrath, M. J., Nieminen, T., Olenius, T., Onnela, A., Petäjä, T., Riccobono, F., Riipinen, I., Rissanen, M., Rondo, L., Ruuskanen, T., Santos, F. D., Sarnela, N., Schallhart, S., Schnitzhofer, R., Seinfeld, J. H., Simon, M., Sipilä, M., Stozhkov, Y., Stratmann, F., Tomé, A., Tröstl, J., Tsagkogeorgas, G., Vaattovaara, P., Viisanen, Y., Virtanen, A., Vrtala, A., Wagner, P. E., Weingartner, E., Wex, H., Williamson, C., Wimmer, D., Ye, P., Yli-Juuti, T., Carslaw, K. S., Kulmala, M., Curtius, J., Baltensperger, U., Worsnop, D. R., Vehkämäki, H. and Kirkby, J.: Molecular understanding of sulphuric acid-amine particle nucleation in the atmosphere., *Nature*, 502(7471), 359–63, doi:10.1038/nature12663, 2013.

15

16

17

18

19

20

21

22

23

24

25

26

27 Angelino, S., Suess, D. T. and Prather, K. A.: Formation of aerosol particles from reactions of secondary and tertiary alkylamines: Characterization by aerosol time-of-flight mass spectrometry, *Environ. Sci. Technol.*, 35(15), 3130–3138, doi:10.1021/es0015444, 2001.

28

29

30

31 Ault, A. P., Moffet, R. C., Baltrusaitis, J., Collins, D. B., Ruppel, M. J., Cuadra-Rodriguez, L. A., Zhao, D., Guasco, T. L., Ebbin, C. J., Geiger, F. M., Bertram, T. H., Prather, K. A. and Grassian, V. H.: Size-dependent changes in sea spray aerosol composition and properties with different seawater conditions, *Environ. Sci. Technol.*, 47(11), 5603–5612, doi:10.1021/es400416g, 2013.

32

33

34

35

36 Barsanti, K. C., McMurry, P. H. and Smith, J. N.: The potential contribution of organic salts to new particle growth, *Atmos. Chem. Phys.*, 9(9), 2949–2957, doi:10.5194/acp-9-2949-2009, 2009.

37

38

39 Berndt, T., Stratmann, F., Sipilä, M., Vanhanen, J., Petäjä, T., Mikkilä, J., Grüner, A., Spindler, G., Lee Mauldin III, R., Curtius, J., Kulmala, M. and Heintzenberg, J.: Laboratory study on new particle formation from the reaction OH + SO<sub>2</sub>: influence of experimental conditions, H<sub>2</sub>O vapour, NH<sub>3</sub> and the amine tert-butylamine on the overall process, *Atmos. Chem. Phys.*, 10, 7101–7116, doi:10.5194/acp-10-7101-2010, 2010.

40

41

42

43

44 Berndt, T., Sipilä, M., Stratmann, F., Petäjä, T., Vanhanen, J., Mikkilä, J., Patokoski, J., Taipale, R., Mauldin, R. L. and Kulmala, M.: Enhancement of atmospheric H<sub>2</sub>SO<sub>4</sub>/H<sub>2</sub>O nucleation: Organic oxidation products versus amines, *Atmos. Chem. Phys.*, 14(2), 751–764, doi:10.5194/acp-14-751-2014, 2014.

45

46

47

48 Boucher, O., Randall, D., Artaxo, P., Bretherton, C., Feingold, G., Forster, P., Kerminen, V.-M., Kondo, Y., Liao, H., Lohmann, U., Rasch, P., Satheesh, S. K., Sherwood, S., Stevens, B. and Zhang, X. Y.: Clouds and Aerosols. In: Climate Change 2013: The Physical Science Basis. Contribution of Working Group I to the Fifth Assessment Report of the Intergovernmental Panel on Climate Change, Cambridge, United Kingdom and New York, NY, USA, 87 pp., 2013.

49

50

51

52

53

54 Bzdek, B. R., Ridge, D. P. and Johnston, M. V.: Amine exchange into ammonium bisulfate and ammonium nitrate nuclei, *Atmos. Chem. Phys.*, 10, 3495–3503, doi:10.5194/acp-3495-2010, 2010.

55

56

57 Bzdek, B. R., Ridge, D. P. and Johnston, M. V.: Amine reactivity with charged sulfuric acid clusters, *Atmos. Chem. Phys.*, 11(16), 8735–8743, doi:10.5194/acp-11-8735-2011, 2011.

58

59 Cadle, S. H. and Mulawa, P. A.: Low-molecular-weight aliphatic amines in exhaust from catalyst-equipped cars.,

1 Environ. Sci. Technol., 14(6), 718–723, doi:10.1021/es60166a011, 1980.

2

3 Capes, G., Johnson, B., McFiggans, G., Williams, P. I., Haywood, J. and Coe, H.: Aging of biomass burning  
4 aerosols over West Africa: Aircraft measurements of chemical composition, microphysical properties, and  
5 emission ratios, *J. Geophys. Res. Atmos.*, 113(23), 1–13, doi:10.1029/2008JD009845, 2008.

6

7 Christie, A. O. and Crisp, D. J.: Activity coefficients of the n-primary, secondary and tertiary aliphatic amines in  
8 aqueous solution, *J. Appl. Chem.*, 17, 1967.

9

10 Chang, I.-H., Lee, C.-G. and Lee, D. S.: Development of an automated method for simultaneous determination of  
11 low molecular weight aliphatic amines and ammonia in ambient air by diffusion scrubber coupled to ion  
12 chromatography, *Anal. Chem.*, 75(22), 6141–6146, doi:10.1021/ac0347314, 2003.

13

14 Creamean, J. M., Ault, A. P., Ten Hoeve, J. E., Jacobson, M. Z., Roberts, G. C., Prather, K. A., Hoeve, J. E. Ten,  
15 Jacobson, Z., Roberts, G. C. and Prather, K. A.: Measurements of aerosol chemistry during new particle formation  
16 events at a remote rural mountain site, *Environ. Sci. Technol.*, 45(19), 8208–8216, doi:10.1021/es103692f, 2011.

17

18 Dabek-Zlotorzynska, E. and Maruszak, W.: Determination of dimethylamine and other low-molecular-mass  
19 amines using capillary electrophoresis with laser-induced fluorescence detection., *J. Chromatogr. B. Biomed. Sci.*  
20 *Appl.*, 714(1), 77–85, 1998.

21

22 Dall’Osto, M., Ceburnis, D., Monahan, C., Worsnop, D. R., Bialek, J., Kulmala, M., Kurtén, T., Ehn, M., Wenger,  
23 J., Sodeau, J., Healy, R. and O’Dowd, C.: Nitrogenated and aliphatic organic vapors as possible drivers for marine  
24 secondary organic aerosol growth, *J. Geophys. Res. Atmos.*, 117(12), 1-10, doi:10.1029/2012JD017522, 2012.

25

26 Dawson, M. L., Perraud, V., Gomez, a., Arquero, K. D., Ezell, M. J. and Finlayson-Pitts, B. J.: Measurement of  
27 gas-phase ammonia and amines in air by collection onto an ion exchange resin and analysis by ion  
28 chromatography, *Atmos. Meas. Tech.*, 7(2), 1573–1602, doi:10.5194/amt-7-2733-2014, 2014.

29

30 Denkenberger, K. A., Moffet, R. C., Holecek, J. C., Rebotier, T. P. and Prather, K. A.: Real-time, single-particle  
31 measurements of oligomers in aged ambient aerosol particles, *Environ. Sci. Technol.*, 41(15), 5439–5446,  
32 doi:10.1021/es0703291, 2007.

33

34 Di Lorenzo, R. A. and Young, C. J.: Size separation method for absorption characterization in brown carbon:  
35 Application to an aged biomass burning sample, *Geophys. Res. Lett.*, 43(1), 458–465,  
36 doi:10.1002/2015GL066954, 2016.

37

38 Di Lorenzo, R. A., Washenfelder, R. A., Attwood, A. R., Guo, H., Xu, L., Ng, N. L., Weber, R. J., Baumann, K.,  
39 Edgerton, E. and Young, C. J.: Molecular size separated brown carbon absorption for fresh and aged biomass  
40 burning plumes at multiple field sites, *Environ. Sci. Technol. (under review)*, 2016.

41

42 Ehn, M., Thornton, J. A., Kleist, E., Sipilä, M., Junninen, H., Pullinen, I., Springer, M., Rubach, F., Tillmann, R.,  
43 Lee, B., Lopez-Hilfiker, F., Andres, S., Acir, I.-H., Rissanen, M., Jokinen, T., Schobesberger, S., Kangasluoma,  
44 J., Kontkanen, J., Nieminen, T., Kurtén, T., Nielsen, L. B., Jørgensen, S., Kjaergaard, H. G., Canagaratna, M.,  
45 Maso, M. D., Berndt, T., Petäjä, T., Wahner, A., Kerminen, V.-M., Kulmala, M., Worsnop, D. R., Wildt, J. and  
46 Mentel, T. F.: A large source of low-volatility secondary organic aerosol, *Nature*, 506(7489), 476–479,  
47 doi:10.1038/nature13032, 2014.

48

49 Erupe, M. E., Liberman-Martin, A., Silva, P. J., Malloy, Q. G. J., Yonis, N., Cocker, D. R. and Purvis-Roberts, K.  
50 L.: Determination of methylamines and trimethylamine-N-oxide in particulate matter by non-suppressed ion  
51 chromatography, *J. Chromatogr. A*, 1217(13), 2070–2073, doi:10.1016/j.chroma.2010.01.066, 2010.

52

53 Erupe, M. E., Viggiano, a. a. and Lee, S. H.: The effect of trimethylamine on atmospheric nucleation involving  
54  $H_2SO_4$ , *Atmos. Chem. Phys.*, 11(10), 4767–4775, doi:10.5194/acp-11-4767-2011, 2011.

55

56 Facchini, M. C., Decesari, S., Rinaldi, M., Carbone, C., Finessi, E., Mircea, M., Fuzzi, S., Moretti, F., Tagliavini,  
57 E., Ceburnis, D. and O’Dowd, C. D.: Important source of marine secondary organic aerosol from biogenic amines.,  
58 *Environ. Sci. Technol.*, 42(24), 9116–9121, doi:10.1021/es8018385, 2008.

59

1 Fekete, A., Frommberger, M., Ping, G., Lahaniatis, M. R., Lintelman, J., Fekete, J., Gebefugi, I., Malik, A. K.,  
2 Kettrup, A. and Schmitt-Kopplin, P.: Development of a capillary electrophoretic method for the analysis of low-  
3 molecular-weight amines from metal working fluid aerosols and ambient air, *Electrophoresis*, 27(5–6), 1237–  
4 1247, doi:10.1002/elps.200500724, 2006.

5 Fournier, M., Lesage, J., Ostiguy, C. and Tra, H. Van: Sampling and analytical methodology development for the  
6 determination of primary and secondary low molecular weight amines in ambient air, *J Env. Monit*, 10(3), 379–  
7 386, doi:10.1039/b719091n, 2008.

8 Ge, X., Wexler, A. S. and Clegg, S. L.: Atmospheric amines - Part I. A review, *Atmos. Environ.*, 45(3), 524–546,  
9 doi:10.1016/j.atmosenv.2010.10.012, 2011.

10 Gibb, S. W., Mantoura, R. F. C., Liss, P. S. and Barlow, R. G.: Distributions and biogeochemistries of  
11 methylamines and ammonium in the Arabian Sea, *Deep. Res. Part II Top. Stud. Oceanogr.*, 46(3–4), 593–615,  
12 doi:10.1016/S0967-0645(98)00119-2, 1999a.

13 Gibb, S. W., Mantoura, R. F. C. and Liss, P. S.: Ocean-atmosphere exchange and atmospheric speciation of  
14 ammonia and methylamines in the region of the NW Arabian Sea, *Global Biogeochem. Cycles*, 13(1), 161–178,  
15 doi:10.1029/98GB00743, 1999b.

16 Gorzelska, K. and Galloway, J. N.: Amine nitrogen in the atmospheric environment over the North Atlantic Ocean,  
17 *Global Biogeochem. Cycles*, 4(3), 309–333, doi:10.1029/GB004i003p00309, 1990.

18 Hatsis, P. and Lucy, C. A.: Evaluation of column temperature as a means to alter selectivity in the cation exchange  
19 separation of alkali metals, alkaline earth metals and amines., *Analyst*, 126(12), 2113–2118,  
20 doi:10.1039/b106639k, 2001.

21 Healy, R. M., Evans, G. J., Murphy, M., Sierau, B., Arndt, J., McGillicuddy, E., O'Connor, I. P., Sodeau, J. R. and  
22 Wenger, J. C.: Single-particle speciation of alkylamines in ambient aerosol at five European sites, *Anal. Bioanal.*  
23 *Chem.*, 407(20), 5899–5909, doi:10.1007/s00216-014-8092-1, 2015.

24 Hodshire, A. L., Lawler, M. J., Zhao, J., Ortega, J., Jen, C., Yli-Juuti, T., Brewer, J. F., Kodros, J. K., Barsanti, K.  
25 C., Hanson, D. R., McMurry, P. H., Smith, J. N. and Pierce, J. R.: Multiple new-particle growth pathways observed  
26 at the US DOE Southern Great Plains field site, *Atmos. Chem. Phys.*, 16, 9321–9348, doi:10.5194/acp-16-9321-  
27 2016, 2016.

28 Huang, G., Hou, J. and Zhou, X.: A measurement method for atmospheric ammonia and primary amines based on  
29 aqueous sampling, OPA derivatization and HPLC analysis, *Environ. Sci. Technol.*, 43(15), 5851–5856,  
30 doi:10.1021/es900988q, 2009.

31 Huang, R. J., Li, W. B., Wang, Y. R., Wang, Q. Y., Jia, W. T., Ho, K. F., Cao, J. J., Wang, G. H., Chen, X., Ei  
32 Haddad, I., Zhuang, Z. X., Wang, X. R., Prèvôt, A. S. H., O'Dowd, C. D. and Hoffmann, T.: Determination of  
33 alkylamines in atmospheric aerosol particles: A comparison of gas chromatography-mass spectrometry and ion  
34 chromatography approaches, *Atmos. Meas. Tech.*, 7(7), 2027–2035, doi:10.5194/amt-7-2027-2014, 2014.

35 Hudson, P. K., Murphy, D. M., Cziczo, D. J., Thomson, D. S., de Gouw, J. A., Warneke, C., Holloway, J., Jost,  
36 H. J. and Hübner, G.: Biomass-burning particle measurements: Characteristics composition and chemical  
37 processing, *J. Geophys. Res. D Atmos.*, 109(23), 1–11, doi:10.1029/2003JD004398, 2004.

38 IARC Monographs on the Evaluation of Carcinogenic Risks to Humans: Outdoor Air Pollution (World Health  
39 Organization), <http://monographs.iarc.fr/ENG/Classification> (accessed Aug 9, 2016), 2016.

40 Jen, C. N., Zhao, J., McMurry, P. H. and Hanson, D. R.: Chemical ionization of clusters formed from sulfuric acid  
41 and dimethylamine or diamines, *Atmos. Chem. Phys. Discuss.*, 0, 1–20, doi:10.5194/acp-2016-492, 2016a.

42 Jen, C. N., Bachman, R., Zhao, J., McMurry, P. H. and Hanson, D. R.: Diamine-sulfuric acid reactions are a potent  
43 source of new particle formation, , 867–873, doi:10.1002/2015GL066958.Received, 2016b.

44 Key, D., Stihle, J., Petit, J.-E., Bonnet, C., Depernon, L., Liu, O., Kennedy, S., Latimer, R., Burgoyne, M., Wanger,  
45 D., Webster, A., Casunuran, S., Hidalgo, S., Thomas, M., Moss, J. A. and Baum, M. M.: Integrated method for the  
46

1 measurement of trace nitrogenous atmospheric bases, *Atmos. Meas. Tech.*, 4(12), 2795–2807, doi:10.5194/amt-  
2 4-2795-2011, 2011.

3 Kovac, N., Glavas, N., Dolenec, M., Smuc, N. R. and Slejkovec, Z.: Chemical Composition of Natural Sea Salt  
4 from the Secovlje Salina (Gulf of Trieste, northern Adriatic), *Acta Chim. Slov.*, 60(3), 706–714, 2013.

5

6 Kuhn, U., Sintermann, J., Spirig, C., Jocher, M., Ammann, C. and Neftel, a.: Basic biogenic aerosol precursors:  
7 Agricultural source attribution of volatile amines revised, *Geophys. Res. Lett.*, 38(16), 1–8,  
8 doi:10.1029/2011GL047958, 2011.

9

10 Kulisa, K.: The effect of temperature on the cation-exchange separations in ion chromatography and the  
11 mechanism of zone spreading, *Chem. Anal.*, 49, 665, doi:10.1365/s10337-005-0545-4, 2004.

12

13 Kulmala, M., Kontkanen, J., Junninen, H., Lehtipalo, K., Manninen, H. E., Nieminen, T., Petäjä, T., Sipilä, M.,  
14 Schobesberger, S., Rantala, P., Franchin, A., Jokinen, T., Järvinen, E., Äijälä, M., Kangasluoma, J., Hakala, J.,  
15 Aalto, P. P., Paasonen, P., Mikkilä, J., Vanhanen, J., Aalto, J., Hakola, H., Makkonen, U., Ruuskanen, T., Mauldin,  
16 R. L., Duplissy, J., Vehkämäki, H., Bäck, J., Kortelainen, A., Riipinen, I., Kurtén, T., Johnston, M. V., Smith, J.  
17 N., Ehn, M., Mentel, T. F., Lehtinen, K. E. J., Laaksonen, A., Kerminen, V.-M. and Worsnop, D. R.: Direct  
18 observations of atmospheric aerosol nucleation., *Science*, 339(6122), 943–6, doi:10.1126/science.1227385, 2013.

19

20 Kurtén, T., Loukonen, V., Vehkämäki, H. and Kulmala, M.: Amines are likely to enhance neutral and ion-induced  
21 sulfuric acid-water nucleation in the atmosphere more effectively than ammonia, *Atmos. Chem. Phys.*, 8, 4095–  
22 4103, doi:10.5194/acp-8-4095-2008, 2008.

23

24 Kürten, A., Bergen, A., Heinritzi, M., Leiminger, M., Lorenz, V., Piel, F., Simon, M., Sitals, R., Wagner, A. and  
25 Curtius, J.: Observation of new particle formation and measurement of sulfuric acid, ammonia, amines and highly  
26 oxidized molecules using nitrate CI-APi-TOF at a rural site in central Germany, *Atmos. Chem. Phys. Discuss.*,  
27 0(June), 1–47, doi:10.5194/acp-2016-294, 2016.

28

29 Kuwata, K., Akiyama, E., Yamasaki, H., Kuge, Y. and Kisa, Y.: Trace determination of low molecular weight  
30 aliphatic amines in air by gas chromatography, *Anal. Chem.*, 55, 2199–2201, 1983.

31

32 Leach, J., Blanch, A. and Bianchi, A. C.: Volatile organic compounds in an urban airborne environment adjacent  
33 to a municipal incinerator, waste collection centre and sewage treatment plant, *Atmos. Environ.*, 33(26), 4309–  
34 4325, doi:10.1016/S1352-2310(99)00115-6, 1999.

35

36 Li, F., Liu, H., Xue, C., Xin, X., Xu, J., Chang, Y., Xue, Y. and Yin, L.: Simultaneous determination of  
37 dimethylamine, trimethylamine and trimethylamine-n-oxide in aquatic products extracts by ion chromatography  
38 with non-suppressed conductivity detection, *J. Chromatogr. A*, 1216(31), 5924–5926,  
39 doi:10.1016/j.chroma.2009.06.038, 2009.

40

41 Lloyd, J. A., Heaton, K. J. and Johnston, M. V.: Reactive uptake of trimethylamine into ammonium nitrate  
42 particles, *J. Phys. Chem. A*, 113(17), 4840–4843, doi:10.1021/jp900634d, 2009.

43

44 Lobert, J. M., Scharffe, D. H., Hao, W. M. and Crutzen, P. J.: Importance of biomass burning in the atmospheric  
45 budgets of nitrogen-containing gases, *Nature*, 346(6284), 552–554, doi:10.1038/346552a0, 1990.

46

47 Lohmann, U. and Feichter, J.: Global indirect aerosol effects: a review, *Atmos. Chem. Phys.*, 5, 715–737,  
48 doi:10.5194/acp-5-715-2005, 2005.

49

50 Loukonen, V., Kurtén, T., Ortega, I. K., Vehkämäki, H., Pádua, A. A. H., Sellegrí, K. and Kulmala, M.: Enhancing  
51 effect of dimethylamine in sulfuric acid nucleation in the presence of water – a computational study, *Atmos. Chem.*  
52 *Phys.*, 10, 4961–4974, doi:10.5194/acp-10-4961-2010, 2010.

53

54 Loukonen, V., Kuo, I. F. W., McGrath, M. J. and Vehkämäki, H.: On the stability and dynamics of (sulfuric  
55 acid)(ammonia) and (sulfuric acid)(dimethylamine) clusters: A first-principles molecular dynamics investigation,  
56 *Chem. Phys.*, 428, 164–174, doi:10.1016/j.chemphys.2013.11.014, 2014.

57

58 Lunn, F. and Van de Vyver, J.: Sampling and analysis of air in pig houses, *Agric. Environ.*, 3, 159–169,

1 doi:10.1016/0304-1131(77)90007-8, 1977.  
2

3 Mader, B. T.: Molecular composition of the water-soluble fraction of atmospheric carbonaceous aerosols collected  
4 during ACE-Asia, *J. Geophys. Res.*, 109(D6), 1–13, doi:10.1029/2003JD004105, 2004.

5

6 Müller, C., Iinuma, Y., Karstensen, J., van Pinxteren, D., Lehmann, S., Gnauk, T. and Herrmann, H.: Seasonal  
7 variation of aliphatic amines in marine sub-micrometer particles at the Cape Verde islands, *Atmos. Chem. Phys.*  
8 *Discuss.*, 9(4), 14825–14855, doi:10.5194/acpd-9-14825-2009, 2009.

9

10 Murphy, S. M., Sorooshian, A., Kroll, J. H., Ng, N. L., Chhabra, P., Tong, C., Surratt, J. D., Knipping, E., Flagan,  
11 R. C. and Seinfeld, J. H.: Secondary aerosol formation from atmospheric reactions of aliphatic amines, *Atmos.*  
12 *Chem. Phys.*, 7, 2313–2337, doi:10.5194/acp-7-2313-2007, 2007.

13

14 Myhre, G., Shindell, D., Bréon, F.-M., Collins, W., Fuglestvedt, J., Huang, J., Koch, D., Lamarque, J.-F., Lee, D.,  
15 Mendoza, B., Nakajima, T., Robock, A., Stephens, G., Takemura, T. and Zhang, H.: Anthropogenic and Natural  
16 Radiative Forcing. In: *Climate Change 2013: The Physical Science Basis. Contribution of Working Group I to the*  
17 *Fifth Assessment Report of the Intergovernmental Panel on Climate Change*, Cambridge, United Kingdom and  
18 New York, NY, USA, 81 pp., 2013.

19

20 Nadykto, A., Herb, J., Yu, F., Xu, Y. and Nazarenko, E.: Estimating the lower limit of the impact of amines on  
21 nucleation in the Earth's atmosphere, *Entropy*, 17(5), 2764–2780, doi:10.3390/e17052764, 2015.

22

23 Ortega, I. K., Kupiainen, O., Kurtén, T., Olenius, T., Wilkman, O., McGrath, M. J., Loukonen, V. and Vehkamäki,  
24 H.: From quantum chemical formation free energies to evaporation rates, *Atmos. Chem. Phys.*, 12(1), 225–235,  
25 doi:10.5194/acp-12-225-2012, 2012.

26

27 Ortega, I. K., Donahue, N. M., Kurtén, T., Kulmala, M., Focsa, C. and Vehkamäki, H.: Can highly oxidized  
28 organics contribute to atmospheric new particle formation?, *J. Phys. Chem. A*, 120(9), 1452–1458,  
29 doi:10.1021/acs.jpca.5b07427, 2016.

30

31 van Pinxteren, M., Fiedler, B., van Pinxteren, D., Iinuma, Y., Kötzinger, A. and Herrmann, H.: Chemical  
32 characterization of sub-micrometer aerosol particles in the tropical Atlantic Ocean: marine and biomass burning  
33 influences, *J. Atmos. Chem.*, 105–125, doi:10.1007/s10874-015-9307-3, 2015.

34

35 Pósfai, M., Simonics, R., Li, J., Hobbs, P. V and Buseck, P. R.: Individual aerosol particles from biomass burning  
36 in southern Africa: 1. Compositions and size distributions of carbonaceous particles, *J. Geophys. Res. Atmos.*,  
37 108(D13), n/a-n/a, doi:10.1029/2002JD002291, 2003.

38

39 Possanzini, M. and Di Palo, V.: Improved HPLC determination of aliphatic amines in air by diffusion and  
40 derivatization techniques, *Chromatographia*, 29(3–4), 151–154, doi:10.1007/BF02268702, 1990.

41

42 Qiu, C., Wang, L., Lal, V., Khalizov, A. F. and Zhang, R.: Heterogeneous reactions of alkylamines with  
43 ammonium sulfate and ammonium bisulfate, *Environ. Sci. Technol.*, 45(11), 4748–4755, doi:10.1021/es1043112,  
44 2011.

45

46 Qiu, C. and Zhang, R.: Multiphase chemistry of atmospheric amines., *Phys. Chem. Chem. Phys.*, 15(16), 5738–  
47 52, doi:10.1039/c3cp43446j, 2013.

48

49 Rabaud, N. E., Ebeler, S. E., Ashbaugh, L. L. and Flocchini, R. G.: Characterization and quantification of odorous  
50 and non-odorous volatile organic compounds near a commercial dairy in California, *Atmos. Environ.*, 37(7), 933–  
51 940, doi:10.1016/S1352-2310(02)00970-6, 2003.

52

53 Rey, M. A. and Pohl, C. A.: Novel cation column for separation of amines and six common inorganic cations. *J.*  
54 *Chrom. A.*, 739, 87–97, 1996.

55

56 Rey, M. and Pohl, C.: Novel cation-exchange column for the separation of hydrophobic and/or polyvalent amines,  
57 *J. Chromatogr. A*, 997(1–2), 199–206, doi:10.1016/S0021-9673(03)00113-4, 2003.

58

Rogge, W. F., Hildemann, L. M., Mazurek, M. a, Cass, G. R. and Simonelt, B. R. T.: Sources of fine organic  
aerosol. 1. Charbroilers and Meat Cooking Operations, *Environ. Sci. Technol.*, 25(6), 1112–1125,

1 doi:10.1021/es00018a015, 1991.  
2

3 Ruiz-Jimenez, J., Parshintsev, J., Laitinen, T., Hartonen, K., Petäjä, T., Kulmala, M. and Riekkola, M. L.: Influence  
4 of the sampling site, the season of the year, the particle size and the number of nucleation events on the chemical  
5 composition of atmospheric ultrafine and total suspended particles, *Atmos. Environ.*, 49, 60–68,  
6 doi:10.1016/j.atmosenv.2011.12.032, 2012.  
7

8 Saleh, R., Robinson, E. S., Tkacik, D. S., Ahern, A. T., Liu, S., Aiken, A. C., Sullivan, R. C., Presto, A. A., Dubey,  
9 M. K., Yokelson, R. J., Donahue, N. M. and Robinson, A. L.: Brownness of organics in aerosols from biomass  
10 burning linked to their black carbon content, *Nat. Geosci.*, 7, 1–4, doi:10.1038/ngeo2220, 2014.  
11

12 Schade, G. W. and Crutzen, P. J.: Emission of aliphatic amines from animal husbandry and their reactions:  
13 Potential source of  $\text{N}_2\text{O}$  and HCN, *J. Atmos. Chem.*, 22(3), 319–346, doi:10.1007/BF00696641, 1995.  
14

15 Schauer, J. J., Kleeman, M. J., Cass, G. R. and Simoneit, B. R. T.: Measurement of emissions from air pollution  
16 sources. 1. C1 through C29 organic compounds from meat charbroiling, *Environ. Sci. Technol.*, 33(10), 1566–  
17 1577, doi:10.1021/es980076j, 1999.  
18

19 Schmeltz, I., and Hoffmann, D.: Nitrogen-containing compounds in tobacco and tobacco smoke, *Chemical  
Review*, 77(3), 295–311, doi: 10.1021/cr60307a001, 1977.  
20

21 Seo, S. G., Ma, Z. K., Jeon, J. M., Jung, S. C. and Lee, W. B.: Measurements of key offensive odorants in a fishery  
22 industrial complex in Korea, *Atmos. Environ.*, 45(17), 2929–2936, doi:10.1016/j.atmosenv.2011.01.032, 2011.  
23

24 Silva, P. J., Erupe, M. E., Price, D., Elias, J., Malloy, Q. G. J., Li, Q., Warren, B. and Cocker, D. R.:  
25 Trimethylamine as precursor to secondary organic aerosol formation via nitrate radical reaction in the atmosphere,  
26 *Environ. Sci. Technol.*, 42(13), 4689–4696, doi:10.1021/es703016v, 2008.  
27

28 Smith, J. N., Dunn, M. J., VanReken, T. M., Iida, K., Stolzenburg, M. R., McMurry, P. H. and Huey, L. G.:  
29 Chemical composition of atmospheric nanoparticles formed from nucleation in Tecamac, Mexico: Evidence for  
30 an important role for organic species in nanoparticle growth, *Geophys. Res. Lett.*, 35(4), 2–6,  
31 doi:10.1029/2007GL032523, 2008.  
32

33 Smith, J. N., Barsanti, K. C., Friedli, H. R., Ehn, M., Kulmala, M., Collins, D. R., Scheckman, J. H., Williams, B.  
34 J. and McMurry, P. H.: Observations of aminium salts in atmospheric nanoparticles and possible climatic  
35 implications., *Proc. Natl. Acad. Sci. U. S. A.*, 107(15), 6634–6639, doi:10.1073/pnas.0912127107, 2010.  
36

37 Sobanska, S., Hwang, H., Choël, M., Jung, H. J., Eom, H. J., Kim, H., Barbillat, J. and Ro, C. U.: Investigation of  
38 the chemical mixing state of individual asian dust particles by the combined use of electron probe X-ray  
39 microanalysis and raman microspectrometry, *Anal. Chem.*, 84(7), 3145–3154, doi:10.1021/ac2029584, 2012.  
40

41 Sorooshian, A., Murphy, S. M., Hersey, S., Gates, H., Padro, L. T., Nenes, a., Brechtel, F. J., Jonsson, H., Flagan,  
42 R. C. and Seinfeld, J. H.: Comprehensive airborne characterization of aerosol from a major bovine source, *Atmos.  
43 Chem. Phys.*, 8, 5489–5520, doi:10.5194/acp-8-5489-2008, 2008.  
44

45 Sorooshian, A., Padro, L. T., Nenes, A., Feingold, G., McComiskey, A., Hersey, S. P., Gates, H., Jonsson, H. H.,  
46 Miller, S. D., Stephens, G. L., Flagan, R. C. and Seinfeld, J. H.: On the link between ocean biota emissions, aerosol,  
47 and maritime clouds: Airborne, ground, and satellite measurements off the coast of California, *Global  
48 Biogeochem. Cycles*, 23(4), 1–15, doi:10.1029/2009GB003464, 2009.  
49

50 Stephen and et al.: A comparative risk assessment of burden of disease and injury attributable to 67 risk factors  
51 and risk factor clusters in 21 regions, 1990–2010: a systematic analysis for the Global Burden of Disease Study  
52 2010, *Lancet*, 380(9859), 2224–2260, doi:10.1016/S0140-6736(12)61766-8.A, 2012.  
53

54 Sun, Y., Zhuang, G., Tang, A., Wang, Y. and An, Z.: Chemical Characteristics of  $\text{PM}_{2.5}$  and  $\text{PM}_{10}$  in Haze–Fog  
55 Episodes in Beijing, *Environ. Sci. Technol.*, 40(10), 3148–3155, doi:10.1021/es051533g, 2006.  
56

57 Suzuki, Y., Kawakami, M. and Akasaka, K.:  $^1\text{H}$  NMR application for characterizing water-soluble organic  
58 compounds in urban atmospheric particles, *Environ. Sci. Technol.*, 35(13), 2656–2664, doi:10.1021/es001861a,  
2001.

1 Takahama, S., Schwartz, R. E., Russell, L. M., MacDonald, A. M., Sharma, S. and Leaitch, W. R.: Organic  
2 functional groups in aerosol particles from burning and non-burning forest emissions at a high-elevation  
3 mountain site, *Atmos. Chem. Phys.*, 11(13), 6367–6386, doi:10.5194/acp-11-6367-2011, 2011.

5 Tao, Y., Ye, X., Jiang, S., Yang, X., Chen, J., Xie, Y. and Wang, R.: Effects of amines on particle growth  
6 observed in new particle formation events, *J. Geos. Res. Atmos.*, 121, 1-12, doi: 10.1002/2015JD024245, 2015

7 Tröstl, J., Chuang, W. K., Gordon, H., Heinritzi, M., Yan, C., Molteni, U., Ahlm, L., Frege, C., Bianchi, F.,  
8 Wagner, R., Simon, M., Lehtipalo, K., Williamson, C., Craven, J. S., Duplissy, J., Adamov, A., Almeida, J.,  
9 Flagan, R. C., Franchin, A., Fuchs, C., Guida, R., Gysel, M., Pet, T. and Steiner, G.: The role of low-volatility  
10 organic compounds for initial particle growth in the atmosphere, *Nature*, 1–56, doi:10.1038/nature18271, 2016.

11

12 Vandenboer, T. C., Petroff, A., Markovic, M. Z. and Murphy, J. G.: Size distribution of alkyl amines in continental  
13 particulate matter and their online detection in the gas and particle phase, *Atmos. Chem. Phys.*, 11(9), 4319–4332,  
14 doi:10.5194/acp-11-4319-2011, 2011.

15

16 VandenBoer, T. C., Markovic, M. Z., Petroff, A., Czar, M. F., Borduas, N. and Murphy, J. G.: Ion chromatographic  
17 separation and quantitation of alkyl methylamines and ethylamines in atmospheric gas and particulate matter using  
18 preconcentration and suppressed conductivity detection, *J. Chromatogr. A*, 1252(3), 74–83,  
19 doi:10.1016/j.chroma.2012.06.062, 2012.

20

21 Van Neste, A., Duce, R. A., Lee, C.: Methylamines in the marine atmosphere, *Geophys. Res. Lett.*, 14(7), 711–  
22 714, 1987.

23

24 Verriele, M., Plaisance, H., Depelchin, L., Benchabane, S., Locoge, N. and Meunier, G.: Determination of 14  
25 amines in air samples using midget impingers sampling followed by analysis with ion chromatography in tandem  
26 with mass spectrometry., *J. Environ. Monit.*, 14(2), 402–8, doi:10.1039/c2em10636a, 2012.

27

28 Wang, L., Khalizov, A. F., Zheng, J., Xu, W., Ma, Y., Lal, V. and Zhang, R.: Atmospheric nanoparticles formed  
29 from heterogeneous reactions of organics, *Nat. Geosci.*, 3(4), 238–242, doi:10.1038/ngeo778, 2010a.

30

31 Wang, L., Vinita, L., Khalizov, A. F. and Zhang, R.: Heterogeneous chemistry of alkylamines with sulfuric acid:  
32 Implications for atmospheric formation of alkylaminium sulfates, *Environ. Sci. Technol.*, 44(7), 2461–2465,  
33 doi:10.1021/es9036868, 2010b.

34

35 Willis, M. D., Burkart, J., Thomas, J. L., Köllner, F., Schneider, J., Bozem, H., Hoor, P. M., Aliabadi, A. A.,  
36 Schulz, H., Herber, A. B., Leaitch, W. R. and Abbatt, J. P. D.: Growth of nucleation mode particles in the  
37 summertime Arctic: a case study, *Atmos. Chem. Phys.*, 16, 7663–7679, doi:10.5194/acp-16-7663-2016, 2016.

38

39 Yang, H., Xu, J., Wu, W. S., Wan, C. H. and Yu, J. Z.: Chemical characterization of water-soluble organic aerosols  
40 at Jeju Island collected during ACE-Asia, *Environ. Chem.*, 1(1), 13–17, doi:10.1071/EN04006, 2004.

41

42 Yang, H., Jian, Z. Y., Hang Ho, S. S., Xu, J., Wu, W. S., Chun, H. W., Wang, X., Wang, X. and Wang, L.: The  
43 chemical composition of inorganic and carbonaceous materials in PM<sub>2.5</sub> in Nanjing, China, *Atmos. Environ.*,  
44 39(20), 3735–3749, doi:10.1016/j.atmosenv.2005.03.010, 2005.

45

46 Yao, L., Wang, M.-Y., Wang, X.-K., Liu, Y.-J., Chen, H.-F., Zheng, J., Nie, W., Ding, A.-J., Geng, F.-H., Wang,  
47 D.-F., Chen, J.-M., Worsnop, D. R. and Wang, L.: Detection of atmospheric gaseous amines and amides by a high  
48 resolution time-of-flight chemical ionization mass spectrometer with protonated ethanol reagent ions, *Atmos.*  
49 *Chem. Phys. Discuss.*, 1–32, doi:10.5194/acp-2016-484, 2016.

50

51 Youn, J. S., Crosbie, E., Maudlin, L. C., Wang, Z. and Sorooshian, A.: Dimethylamine as a major alkyl amine  
52 species in particles and cloud water: Observations in semi-arid and coastal regions, *Atmos. Environ.*, 122, 250–  
53 258, doi:10.1016/j.atmosenv.2015.09.061, 2015.

54

55 Yu, H., McGraw, R. and Lee, S. H.: Effects of amines on formation of sub-3 nm particles and their subsequent  
56 growth, *Geophys. Res. Lett.*, 39(2), 2–7, doi:10.1029/2011GL050099, 2012.

57

1 Zauscher, M. D., Wang, Y., Moore, M. J. K., Gaston, C. J. and Prather, K. A.: Air quality impact and  
2 physicochemical aging of biomass burning aerosols during the 2007 San Diego wildfires, *Environ. Sci. Technol.*,  
3 47(14), 7633–7643, doi:10.1021/es4004137, 2013.

4

5 Zhang, Q. and Anastasio, C.: Free and combined amino compounds in atmospheric fine particles (PM<sub>2.5</sub>) and fog  
6 waters from Northern California, *Atmos. Environ.*, 37(16), 2247–2258, doi:10.1016/S1352-2310(03)00127-4,  
7 2003.

8

9 Zhao, J., Smith, J. N., Eisele, F. L., Chen, M., Kuang, C. and McMurry, P. H.: Observation of neutral sulfuric acid-  
10 amine containing clusters in laboratory and ambient measurements, *Atmos. Chem. Phys.*, 11(21), 10823–10836,  
11 doi:10.5194/acp-11-10823-2011, 2011.

12

13 Zollner, J. H., Glasoe, W. A., Panta, B., Carlson, K. K., McMurry, P. H. and Hanson, D. R.: Sulfuric acid  
14 nucleation: Power dependencies, variation with relative humidity, and effect of bases, *Atmos. Chem. Phys.*, 12(10),  
15 4399–4411, doi:10.5194/acp-12-4399-2012, 2012.

16

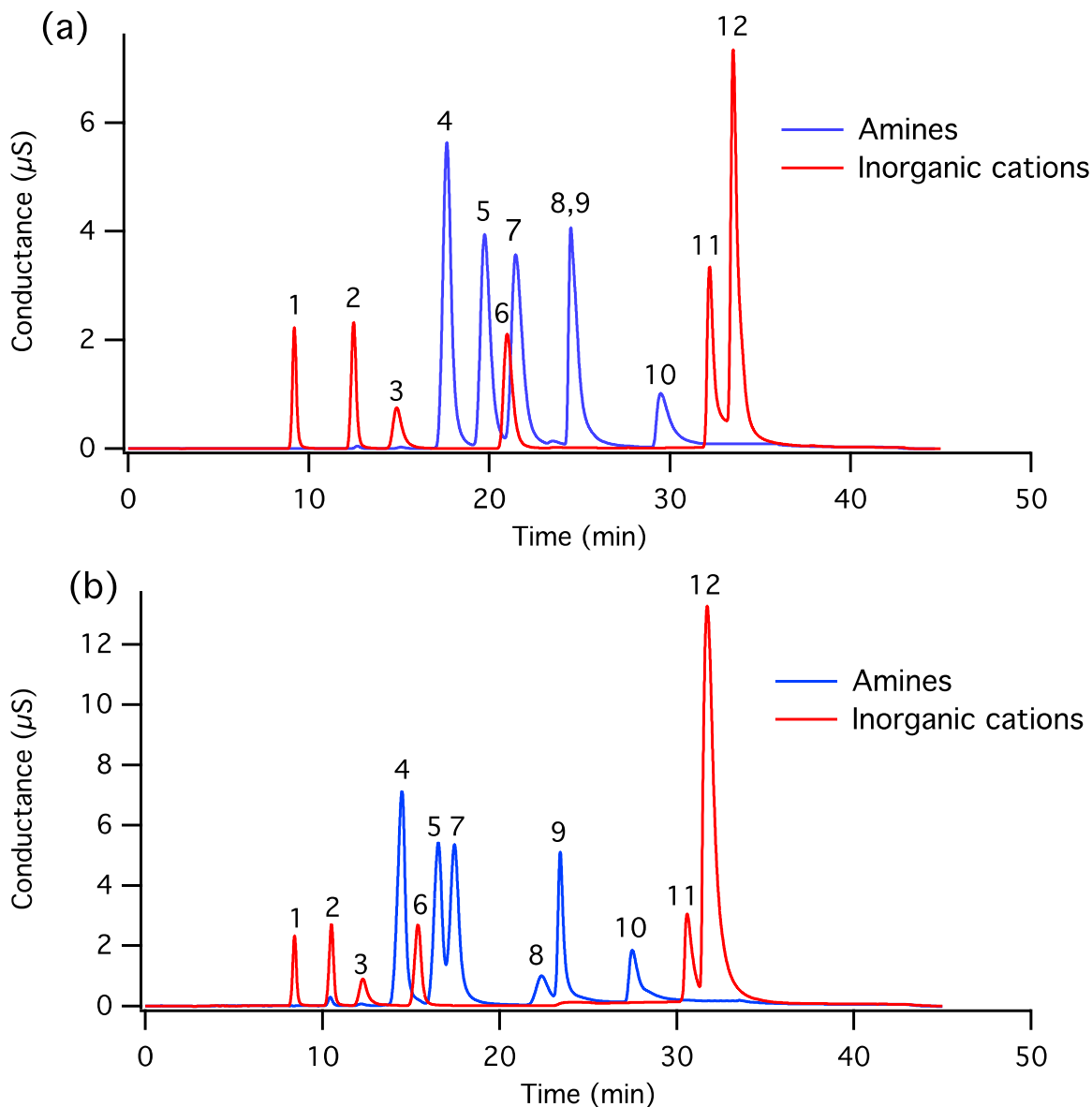
17

18

19

1 Figures

2



3

4

5 Figure 1. Separation of amine and inorganic cation standards with the highest resolution gradient program at (a)  
6 30°C and (b) 55°C. The order of elution and mass of cation injected in (a) is as follows: Li<sup>+</sup> (1, 16 ng), Na<sup>+</sup> (2, 158  
7 ng), NH<sub>4</sub><sup>+</sup> (3, 169 ng), MMAH<sup>+</sup> (4, 500 ng), MEAH<sup>+</sup> (5, 500 ng), K<sup>+</sup> (6, 524 ng), DMAH<sup>+</sup> (7, 500 ng), TMAH<sup>+</sup>  
8 (8, 500 ng), DEAH<sup>+</sup> (9, 500 ng), TEAH<sup>+</sup> (10, 500 ng), Mg<sup>2+</sup> (11, 128 ng), and Ca<sup>2+</sup> (12, 361 ng). Cation peaks  
9 represent the same mass injected and are labeled according to the same numeric identities in (b).

10

11

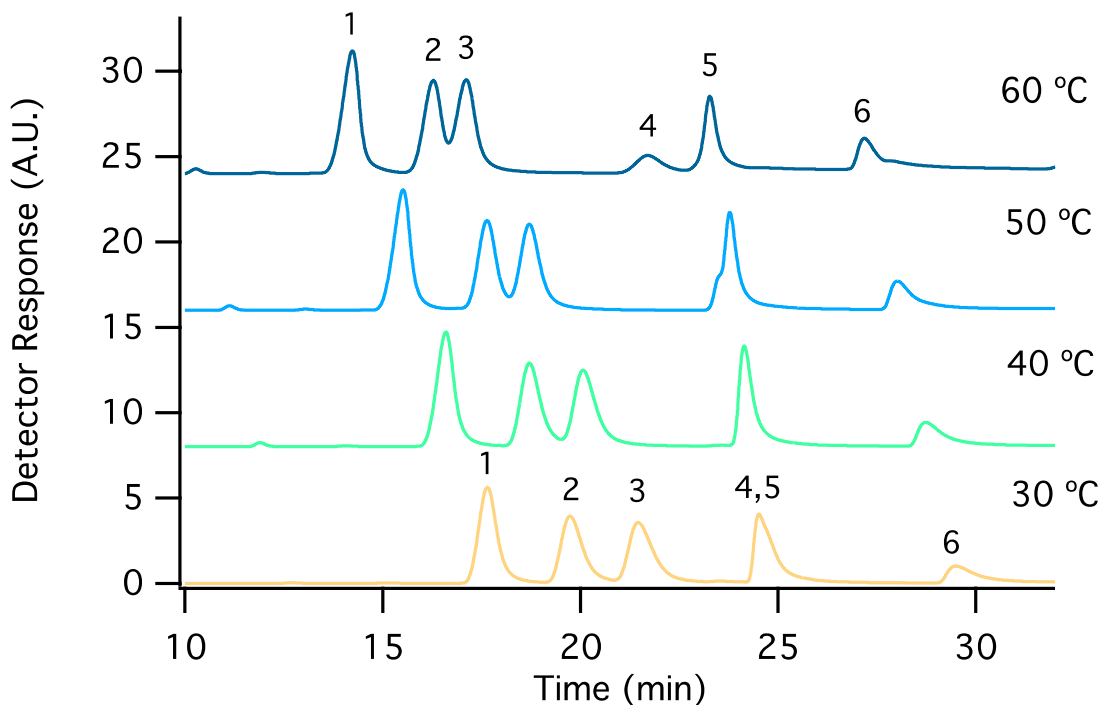
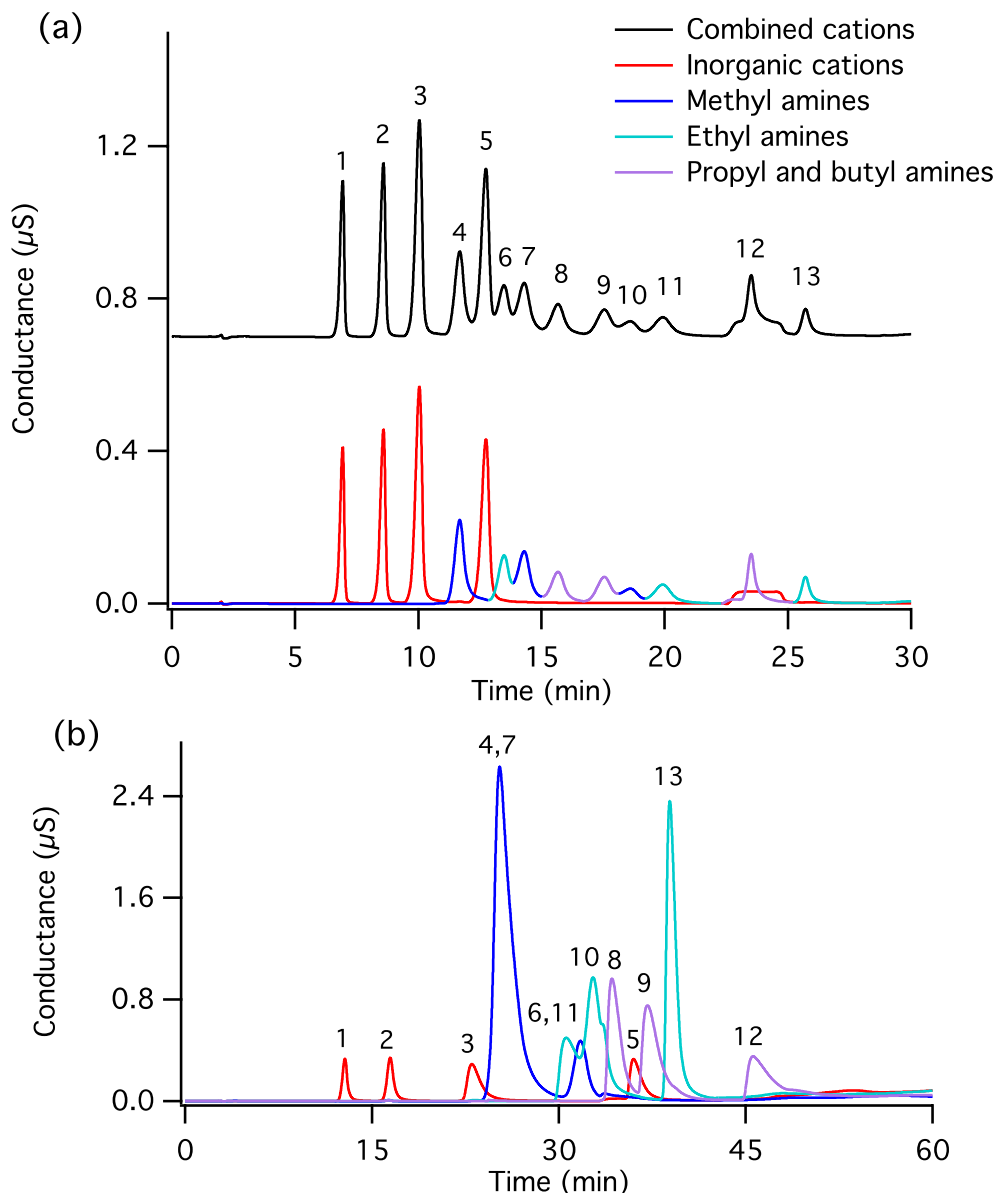


Figure 2. Separation of  $1 \mu\text{g ml}^{-1}$  mixed amines standard with the final method gradient elution program at  $30^\circ\text{C}$ ,  $40^\circ\text{C}$ ,  $50^\circ\text{C}$  and  $60^\circ\text{C}$ . The peak elution order was MMAH $^+$  (1), MEAH $^+$  (2), DMAH $^+$  (3), TMAH $^+$  (4), DEA $^+$  (5), and TEAH $^+$  (6). The separation of diethylamine (DEA) from trimethylamine (TEA) was achieved at column temperatures greater than  $50^\circ\text{C}$ .



1  
2  
3

4 Figure 3. (a) Separation of amine and inorganic cation standards with the addition of  $\text{MPAH}^+$ ,  $\text{iMPAH}^+$  and  
5  $\text{MBAH}^+$  using the final gradient program. The order of elution and mass of cation injected in (a) is as follows:  $\text{Li}^+$   
6 (1, 1.6 ng),  $\text{Na}^+$  (2, 16 ng),  $\text{NH}_4^+$  (3, 17 ng),  $\text{MMAH}^+$  (4, 50 ng),  $\text{K}^+$  (5, 52 ng),  $\text{MEA}^+$  (6, 50 ng),  $\text{DMAH}^+$  (7, 50  
7 ng),  $\text{iMPAH}^+$  (8, 50 ng),  $\text{MPAH}^+$  (9, 50 ng),  $\text{TMAH}^+$  (10, 50 ng),  $\text{DEAH}^+$  (11, 50 ng),  $\text{MBAH}^+$  (12, 50 ng), and  
8  $\text{TEAH}^+$  (13, 50 ng). (b) Separation of amine and inorganic cation standards with the addition of  $\text{MPAH}^+$ ,  $\text{iMPAH}^+$   
9 and  $\text{MBAH}^+$  and the addition of the CG15 column using a modified gradient program. Cation peaks are labeled  
10 accordingly to the same identities in (b) and the mass of analyte injected is as follows:  $\text{Li}^+$  (1.6 ng),  $\text{Na}^+$  (16 ng),  
11  $\text{NH}_4^+$  (17 ng),  $\text{MMAH}^+$  (500 ng),  $\text{K}^+$  (52 ng),  $\text{MEA}^+$  (500 ng),  $\text{DMAH}^+$  (500 ng),  $\text{iMPAH}^+$  (500 ng),  $\text{MPAH}^+$   
12 (500 ng),  $\text{TMAH}^+$  (500 ng),  $\text{DEAH}^+$  (500 ng),  $\text{MBAH}^+$  (500 ng), and  $\text{TEAH}^+$  (500 ng).

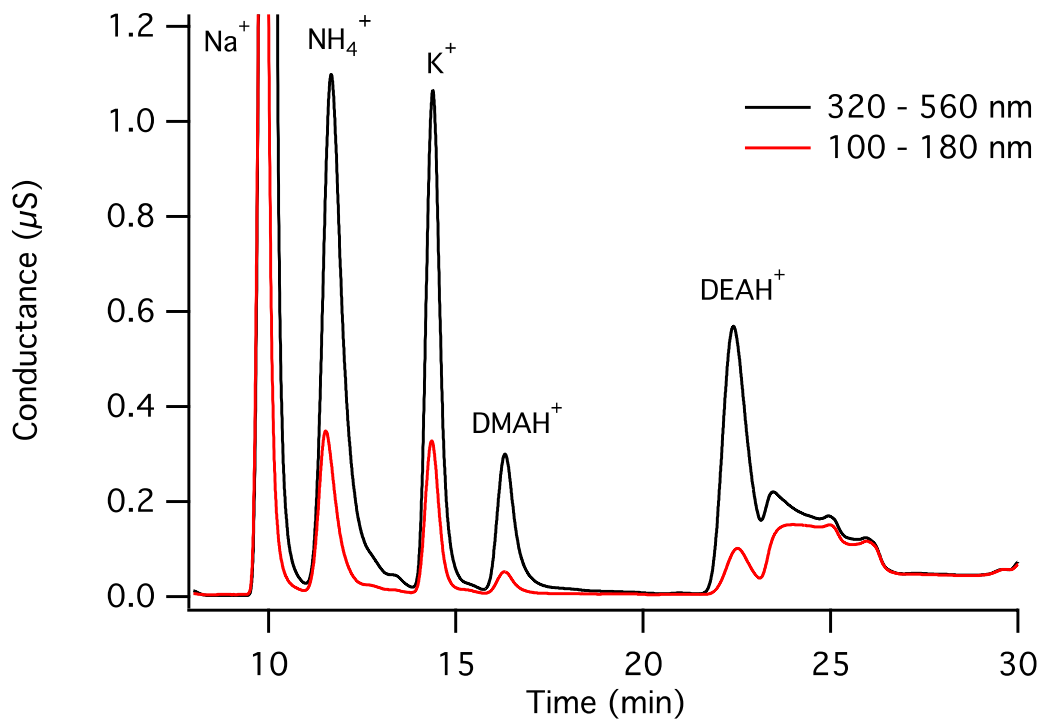
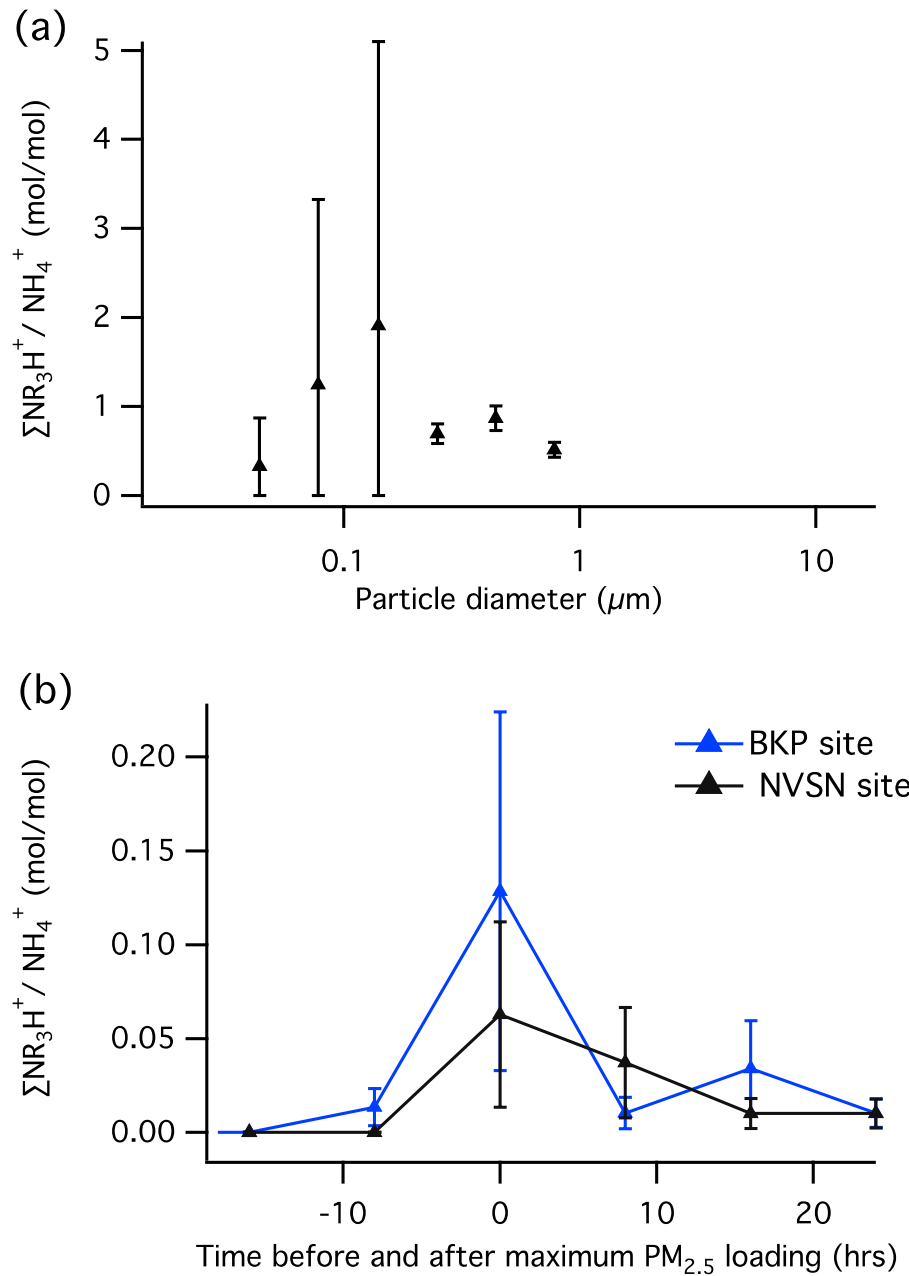


Figure 4. Overlaid chromatograms of MOUDI size-fractionated particle samples collected in St John's on July 6, 2013 during the intrusion of a biomass-burning plume that originated from Northern Labrador and Quebec. The robustness of the separation method for MMAH<sup>+</sup>, DMAH<sup>+</sup> and DEAH<sup>+</sup> from the common inorganic cations is demonstrated for the 320-560 nm (Black) and 100-180 nm (Red) size bins.

1  
2  
3  
4  
5  
6  
7  
8  
9  
10  
11  
12  
13  
14  
15  
16  
17  
18

1



2

3

4 Figure 5. (a) Amines to ammonium ratio in the size-resolved aged biomass-burning sample originating from  
 5 Quebec and Labrador in the summer of 2013. (b) Amines to ammonium ratio for the Burnaby/Kensington Park  
 6 (BKP) site and North Vancouver/Second Narrows (NVSN) site in British Columbia during the summer 2015  
 7 wildfires. The error bars in the graph represent propagated error in the amine and ammonium quantities resulting  
 8 from variability in the field blanks and check standards during the analysis of the samples.

1 Table 1. Separation characteristics and statistics for the CS19 gradient method. The retention time ( $t_r$ ) ranges for the methyl amines, ethyl amines and inorganic cations were  
 2 determined using retention time windows from a full calibration. The peak width and resolution were determined using the highest calibration standards amines (500 ng)  
 3 and inorganic (160 – 520 ng) cations. The  $t_r$  range and peak width were back-calculated for iMPAH<sup>+</sup>, MPAH<sup>+</sup>, MBAH<sup>+</sup>, DABH<sup>+</sup> and DAPH<sup>+</sup> based on the other alkyl amines  
 4 responses to column degradation. Sensitivity, precision, average LOD, and LOD range were analyzed using multiple calibration standards and blanks (see Section 2.4).  
 5 Upper and lower range accuracies were assessed using high and low check standards for the alkyl amines ( $n = 6$ ) and inorganic cations ( $n = 4$ ). The low check standards  
 6 were 15 times more concentrated than the lowest calibration standard and the high check standards were 150 times more concentrated.

Cation	$t_r$ (min)	Peak width (min)	Resolution $n$	Sensitivity ( $\mu\text{S}^* \text{min}^* \text{mol}^{-1}$ )	Precision % ( $\pm 1\sigma$ )	Upper range accuracy (%)	Lower range accuracy (%)	Average LOD (pg) ( $\pm 1\sigma$ )	LOD range (pg)
Li <sup>+</sup>	8.2 – 8.4	0.72	2.68	11.5E08	2	96 $\pm$ 5	82 $\pm$ 4	0.6 $\pm$ 0.2	0.3 - 0.8
Na <sup>+</sup>	10.1 – 10.3	0.73	1.87	5.04E08	2	95 $\pm$ 4	90 $\pm$ 6	8 $\pm$ 4	4 - 14
NH <sub>4</sub> <sup>+</sup>	11.8 – 12.1	1.18	0.65/1.85*	2.45E08	4	103 $\pm$ 4	50 $\pm$ 50	22 $\pm$ 17	7 - 47
MEtAH <sup>+</sup>	12.7 – 13.0	0.99	0.56	2.2E08	---	---	---	3600 ( $n = 1$ )	---
MMAH <sup>+</sup>	13.5 – 13.8	0.86	1.09	1.42E08	5	98 $\pm$ 6	40 $\pm$ 30	300 $\pm$ 300	30 - 650
K <sup>+</sup>	14.7 – 14.8	0.87	1.22	4.14E08	5	99 $\pm$ 2	94 $\pm$ 7	14 $\pm$ 11	4 - 28
MEA <sup>+</sup>	15.5 – 15.8	0.79	1.08	0.90E08	7	97 $\pm$ 5	40 $\pm$ 10	500 $\pm$ 200	200 - 700
DMAH <sup>+</sup>	16.4 – 16.7	0.85	1.64	1.48E08	5	100 $\pm$ 10	30 $\pm$ 30	200 $\pm$ 300	40 - 650
iMPAH <sup>+</sup>	18.2 – 18.5	0.79	2.24	0.84E08	4	90 $\pm$ 10	80 $\pm$ 80	70 $\pm$ 40	40 - 90
MPAH <sup>+</sup>	20.1 – 20.4	0.88	1.55	0.62E08	12	88 $\pm$ 4	90 $\pm$ 90	50 $\pm$ 40	20 - 80
TMAH <sup>+</sup>	21.2 – 21.6	1.11	1.48	0.34E08	16	90 $\pm$ 10	30 $\pm$ 20	600 $\pm$ 300	300 - 1200
DEAH <sup>+</sup>	22.6 – 22.7	1.18	2.51	0.76E08	8	97 $\pm$ 8	50 $\pm$ 30	400 $\pm$ 300	100 - 800
MBAH <sup>+</sup>	25.3 – 25.6	0.43	3.12	0.62E08	1	80 $\pm$ 20	100 $\pm$ 80	910 $\pm$ 30	890 - 930
TEAH <sup>+</sup>	27.3 – 27.7	0.95	3.40	0.85E08	12	96 $\pm$ 4	49 $\pm$ 6	800 $\pm$ 400	500 - 1400
Mg <sup>2+</sup>	30.4 – 30.8	0.79	1.22	12.2E08	1	80 $\pm$ 20	100 $\pm$ 30	2000 $\pm$ 3000	200 - 4000
Ca <sup>2+</sup>	31.6 – 32.9	1.05	3.16	14.3E08	2	90 $\pm$ 20	120 $\pm$ 20	3700 $\pm$ 200	3500 – 3800
DABH <sup>+</sup>	36.6 – 36.9	1.48	0.98	4.5E08	---	---	---	1000 ( $n = 1$ )	---
DAPH <sup>+</sup>	38.0 – 38.4	1.60	N/A	4.9E08	---	---	---	180 ( $n = 1$ )	---

8 resolution calculated for NH<sub>4</sub><sup>+</sup> and MMAH<sup>+</sup>

1 --- = insufficient replicates

